

The Neutron Stars of Soft X-Ray Transients

S. Campana^{1,2}, M. Colpi³, S. Mereghetti⁴, L. Stella^{5,2}, and M. Tavani^{6,4,2}

¹ Osservatorio astronomico di Brera, Via E. Bianchi 46, I-23807 Merate (Lc), Italy

² Affiliated to I.C.R.A.

³ Dipartimento di Fisica, Università degli Studi di Milano, Via Celoria 16, I-20133 Milano, Italy

⁴ Istituto di Fisica Cosmica “G.P.S. Occhialini” del C.N.R., Via Bassini 15, I-20133 Milano, Italy

⁵ Osservatorio astronomico di Monteporzio Catone, Via dell’Osservatorio 2, I-00040 Monteporzio Catone (Roma), Italy

⁶ Columbia Astrophysics Laboratory, Columbia University, New York, NY 10027, USA

Received 4 November 1977; Accepted 20 April 1998

Abstract. Soft X-ray Transients (SXRTs) have long been suspected to contain old, weakly magnetic neutron stars that have been spun up by accretion torques. After reviewing their observational properties, we analyse the different regimes that likely characterise the neutron stars in these systems across the very large range of mass inflow rates, from the peak of the outbursts to the quiescent emission. While it is clear that close to the outburst maxima accretion onto the neutron star surface takes place, as the mass inflow rate decreases, accretion might stop at the magnetospheric boundary because of the centrifugal barrier provided by the neutron star. For low enough mass inflow rates (and sufficiently short rotation periods), the radio pulsar mechanism might turn on and sweep the inflowing matter away. The origin of the quiescent emission, observed in a number of SXRTs at a level of $\sim 10^{32} - 10^{33}$ erg s⁻¹, plays a crucial role in constraining the neutron star magnetic field and spin period. Accretion onto the neutron star surface is an unlikely mechanism for the quiescent emission of SXRTs, as it requires very low magnetic fields and/or long spin periods. Thermal radiation from a cooling neutron star surface in between the outbursts can be ruled out as the only cause of the quiescent emission.

We find that accretion onto the neutron star magnetosphere and shock emission powered by an enshrouded radio pulsar provide far more plausible models. In the latter case the range of allowed neutron star spin periods and magnetic fields is consistent with the values recently inferred from the properties of kHz quasi-periodic oscillation in low mass X-ray binaries. If quiescent SXRTs contain enshrouded radio pulsars, they provide a missing link between X-ray binaries and millisecond pulsars.

Key words: X-ray: binaries – stars: neutron – accretion – pulsars: general

1. Introduction

Transient X-ray sources are quiescent and undetected for most of the time and undergo sporadic outbursts, typically lasting for 10–100 d, during which they emit an intense X-ray flux. They were initially classified on the basis of their spectral hardness, owing to the lack of a clear understanding of their nature (Cominsky et al. 1978). The subsequent discovery of a number of phenomena observed also in different classes of X-ray binaries (e.g. X-ray pulsations and bursts; see e.g. White 1989) showed that there is a close relationship between transient and persistent accreting compact sources. White, Kaluziński & Swank (1984) introduced a revised spectral classification that further extends this analogy. The spectra of *hard* X-ray transients (HXRTs) are characterised by equivalent temperatures $\gtrsim 15$ keV. These sources often contain a young, pulsating, neutron star orbiting a Be star companion and are clearly associated to persistent X-ray pulsars in high mass binaries (Maraschi, Treves & van den Heuvel 1976). The outburst of *soft* X-ray transients (SXRTs), characterised by equivalent temperatures $\lesssim 15$ keV, are often accompanied by a pronounced increase in the luminosity of their (faint) optical counterparts and by the onset of type I burst (thermonuclear flashes on the surface of a neutron star) activity. These properties clearly associate SXRTs with low mass X-ray binaries (LMXRBs) containing an old neutron star. The *ultrasoft* X-ray transients are also associated to LMXRBs, but in this case the similarity with the “high state” spectra of persistent black hole candidates (BHCs), together with the absence of bursts and pulsations, suggests that these systems likely harbor a stellar mass black hole (White & Marshall 1984). This class has been later extended to include also *hard tail* transient sources, based on the analogy with the spectral characteristic of Cyg X-1 in its “low state”. The prediction on the nature of the compact object in different classes of LMXRB transients has been brilliantly confirmed by mass measurements which established A 0620–00, GS 2023+338, GS 1124–68 and GRO J1655–40 as firm BHCs (McClintock & Remillard 1986; Casares, Charles & Naylor 1992; Orsoz et al. 1996) and Cen X-4 as a neutron star (Shahbaz, Naylor & Charles 1993).

Transients systems are characterised by an X-ray luminosity that varies over many decades (variations between 10^{33} and 10^{38} erg s $^{-1}$ are not uncommon). Therefore they allow to investigate accretion onto collapsed stars over a much larger range of luminosities, and therefore accretion rates, than persistent sources. This is well illustrated e.g. by the case of the HXRT EXO 2030+375, a 42 s pulsator, that led to a remarkable progress in the understanding of the physics of accretion onto magnetic neutron stars (Parmar et al. 1989; Parmar, White & Stella 1989; Angelini, Stella & Parmar 1989).

SXRTs, while still poorly studied, provide a unique opportunity to gain crucial insights in the neutron stars that are hosted in non-pulsating LMXRBs. According to current evolutionary scenarios, the neutron stars in transients as well as persistent non-pulsating LMXRBs are gradually spun-up by accretion torques to limiting periods ranging from milliseconds to tens of milliseconds, depending on the value of their residual magnetic field (Alpar et al. 1982; Bhattacharya & van den Heuvel 1991; Phinney & Kulkarni 1994). Once accretion from the companion star stops, the neutron stars in these systems are expected to shine as “recycled” radio pulsars orbiting a low mass companion. These LMXRBs therefore likely represent the progenitors of the weak magnetic field ($10^8 - 10^9$ G) millisecond radio pulsars (MSPs) that are discovered in increasing number in the Galaxy and globular clusters (Backer et al. 1982; Manchester et al. 1991; Taylor, Manchester & Lyne 1993).

Despite numerous searches, fast coherent X-ray pulsations in the persistent emission of LMXRBs directly arising from the neutron star rotation have proved elusive (see e.g. Vaughan et al. 1994 and references therein). Only after the launch of the Rossi X-Ray Timing Explorer (RossiXTE) kiloHertz (kHz) quasi-periodic oscillations (QPOs) have been discovered in several objects (for a review see van der Klis 1997, 1998). In the great majority of the brightest X-ray binaries two kHz QPOs (between 0.3 and 1.2 kHz) have been discovered. These sources are usually classified according to the track in the colour-colour diagram for different luminosities (e.g. Hasinger & van der Klis 1989; van der Klis 1995). Atoll sources (or suspected) usually maintain their frequency difference ($\sim 300 - 500$ Hz) constant over large variations of QPOs centroid frequencies and the centroid frequency appears to be positively correlated with the X-ray luminosity (4U 1728–34 Strohmayer et al. 1996; 4U 0614+091 Ford et al. 1997; KS 1731–260 Wijnands & van der Klis 1997; 4U 1636–53 Wijnands et al. 1997; 4U 1735–44 Wijnands et al. 1998a; 4U 1820–30 Smale, Zhang & White 1997; 4U 1705–44 Ford, van der Klis & Kaaret 1998). A different case is presented by 4U 1608–52 for which a varying peak separation has been observed (Mendez et al. 1998).

In the Z source Sco X-1 (van der Klis et al. 1997) the frequency separation between the kHz QPOs decreases with mass accretion rate, but in the other Z sources (GX 5–1 van der Klis et al. 1996; Cyg X-2 Wijnands et al. 1998b; GX 340+0 Jonker et al. 1998; GX 17+2 Wijnands et al. 1998c) the separation remains approximately constant, although a similar decrease in peak separation as found in Sco X-1 can not be excluded.

Nearly constant pulsations at this frequency difference have also been revealed during X-ray bursts in 4U 1728–34 (2.8 ms; Strohmayer et al. 1996) and during a persistent emission interval of 4U 0614+09 (3.1 ms; Ford et al. 1997). In the case of KS 1731–260 and 4U 1636–53 the frequency difference between the two QPO peaks is consistent with half the frequency of the

nearly periodic signals at ~ 524 and 581 Hz, respectively, that have been detected during type I bursts from these sources (KS 1731–260: Smith, Morgan & Bradt 1997; Wijnands & van der Klis 1997; 4U 1636–53: Zhang et al. 1996a; Wijnands et al. 1997). In Aql X-1 a similar coherent modulation during an X-ray burst has been observed at ~ 550 Hz, whereas only one kHz QPO has been revealed at 750–830 Hz (Zhang et al. 1998).

The most straightforward interpretation of these findings is based on magnetospheric beat-frequency models (Alpar & Shaham 1985; Lamb et al. 1985; Miller, Lamb & Psaltis 1998): the nearly coherent signal during type I bursts corresponds to the spin frequency of the neutron star, whereas the higher frequency kHz QPO arise from the Keplerian motion of matter in the innermost accretion disk region, close to the magnetospheric boundary or at the sonic radius. The lower frequency kHz QPO originates instead from modulated accretion at the beat frequency between the neutron star spin frequency and the Keplerian frequency at the magnetospheric boundary.

These kHz QPOs provide the first evidence that the neutron stars in LMXRBs are spinning at periods of the order of milliseconds and are the likely progenitors of MSPs.

The large accretion rate variations that are characteristic of SXRTs should allow the exploration of a variety of different regimes for the neutron stars in these systems which are inaccessible to persistent LMXRBs. While it is clear that, when in outbursts, SXRTs are powered by accretion, the origin of the low luminosity X-ray emission that has been detected in the quiescent state of several SXRTs is still unclear. An interesting possibility is that a MSP be visible in the quiescent state of SXRTs (Stella et al. 1994; hereafter Paper I). This would provide a “missing link” between persistent LMXRBs and recycled MSPs.

This paper concentrates on various aspects of the physics of the neutron stars in SXRTs. A short account of our main original results has been given in Paper I. After a review of the observations of SXRTs¹ (Section 2, see also Tanaka & Shibazaki 1996), we give a brief description of the models for the outburst mechanism (Section 3). In Section 4 we explore the different regimes that are expected for the neutron stars of SXRTs in the decay phase of their outbursts. In Section 5 we expand on the different emission mechanisms which might be responsible for the quiescent luminosity. The conditions under which the neutron stars of SXRTs evolve towards and remain within the radio pulsar region of the magnetic field – spin period ($B - P$) diagram are discussed in Section 6. The main conclusions of the paper are presented in Section 7.

2. The properties of Soft X-ray Transients

SXRTs are a fairly inhomogeneous class². Often their outbursts consist of a flux increase lasting a few days that reaches X-ray luminosities of $L_X \sim 10^{37} - 10^{38}$ erg s $^{-1}$, followed by a slower, nearly exponential decay with a timescale of weeks to

¹Readers who are familiar with the subject may refer to Table I only.

²Some sources (especially in the vicinity of the Galactic Center) have been classified as transients even if their peak luminosity was only a few times higher than the instrumental detection limit. In the absence of additional evidence for their transient behaviour, these sources should be considered only as variable X-ray sources.

months. Outbursts of this kind have been observed in Cen X-4, Aql X-1, 4U 1730–22 and A 1742–289 (White, Kaluziński & Swank 1984 and references therein) and perhaps in a few other cases (see Table I). Other sources (like EXO 0748–676, 4U 2129+47 and 4U 1608–52), alternate long periods of relatively high (and often variable) X-ray flux with others in which they are detected at a much lower level, if at all. Unfortunately, the transitions between these intensity states have been poorly studied so far. With the possible exception of Aql X-1 (see below), the intervals between outbursts are irregular, often in the 1–10 yr range, but for many sources only one outburst has been observed so far.

Available X-ray data on SXRTs are still sparse: in most cases the outburst monitoring has been carried out with wide field instruments, characterised by limited effective area, energy range and, especially, sensitivity. A relatively small number of pointed observations close to the outburst maxima have been obtained mainly with large area collimated detectors for a few systems, whereas the quiescent emission, months to years away from the outbursts, has been investigated for ~ 10 SXRTs, mainly with low energy X-ray telescopes. At least two SXRTs, Aql X-1 and Cen X-4, have been determined to emit very different spectra in different states. While close to the outburst peak the spectra are relatively soft (equivalent thermal bremsstrahlung temperatures of $kT_{\text{br}} \sim 5$ keV), at intermediate luminosities ($\sim 10^{35} - 10^{37}$ erg s $^{-1}$) during the rise and decay of the outburst, a high energy tail extending to at least ~ 100 keV is detected (a similar tail is also seen in a few persistent burst sources; e.g. Barret & Vedrenne 1994). The evolution at the end of the outburst from luminosities of $\sim 10^{34} - 10^{36}$ erg s $^{-1}$ to quiescence is basically unknown. Only recently, BeppoSAX observations allowed to explore this luminosity range in the case of Aql X-1 (Campana et al. 1998; see Section 2.2.1). The X-ray spectrum of Aql X-1 consists again of a soft component plus a hard energy tail, similar to the one observed at higher luminosities. The spectra in the quiescent state ($L_X \sim 10^{32} - 10^{33}$ erg s $^{-1}$) are characterised by a soft component (equivalent black body temperatures of $kT_{\text{bb}} \sim 0.1 - 0.3$ keV). For those SXRTs observed above a few keV, a power-law like high energy tail has been revealed which, in the case of Aql X-1, hardens as the luminosity decreases below $\sim 10^{33}$ erg s $^{-1}$ (Campana et al. 1998).

Type I X-ray bursts have been observed in the active phase of thirteen SXRTs. These burst of X-ray radiation are most likely due to thermonuclear flashes at the surface of accreting neutron stars (Maraschi & Cavaliere 1977). There is no evidence that these bursts differ in any property from those of persistent LMXRBs (e.g. Lewin, van Paradijs & Taam 1993, 1995), thus supporting the idea that SXRTs contain weakly magnetic neutron stars accreting from a low mass companion.

Up to now three SXRTs (4U 1608–52 Berger et al. 1996; KS 1731–260 Wijnands & van der Klis 1997; Aql X-1 Zhang et al. 1998) have displayed kHz QPOs, when their X-ray luminosity was at a level of $10^{36} - 10^{37}$ erg s $^{-1}$. In the case of 4U 1608–52 the centroid frequency of these QPOs (between 600 and 1100 Hz) does not correlate with the observed X-ray luminosity. For Aql X-1 a single kHz QPO in the same frequency range (750–830 Hz) has been observed at two different luminosities ($1.2 - 1.7 \times 10^{36}$ erg s $^{-1}$). The persistent emission of KS 1731–260 shows twin kHz QPO around 900 and 1160 Hz, respectively. The frequency difference (~ 260 Hz) between these QPOs is consistent with half the frequency of the nearly peri-

odic 524 Hz signal observed in a Type I burst from this source (Smith, Morgan & Bradt 1997; Wijnands & van der Klis 1997). When interpreted in terms of beat-frequency models (Alpar & Shaham 1985; Lamb et al. 1985; Miller, Lamb & Psaltis 1998) these results imply a neutron star spin period of ~ 3.8 ms.

The X-ray outbursts of SXRTs are often accompanied by a considerable enhancement of their optical luminosity (optical novae). Increases up to ~ 6 magnitudes with respect to the quiescent state have been measured, which have greatly helped in the identification of the optical counterparts of seven SXRTs. The optical spectra during outbursts are usually characterised by a rather flat continuum with emission lines (Balmer, He II, N III; van Paradijs & McClintock 1995), similar to those of bright persistent LMXRBs. These spectra result mainly from reprocessing of the high energy photons at the accretion disk and companion star. In some cases, the intrinsic spectrum of the companion star becomes detectable in the quiescent state, therefore making detailed photometric and spectroscopic measurements possible. These studies have shown that SXRTs contain late type stars (G or K), and in some cases allowed a determination of the orbital periods. These are known for seven SXRTs and are in the range from 4 to 19 hr, similar to those of LMXRBs (van Paradijs & McClintock 1994). Only for one SXRT (Cen X-4) the mass function has been measured (Shahbaz, Naylor & Charles 1993).

Radio emission has been observed during the outbursts of A1742–289 (Davis et al. 1976), Aql X-1 (Hjellming, Han & Roussel-Dupré 1990) and Cen X-4 (Hjellming et al. 1988).

SXRTs are located in the galactic plane with a distribution similar to that of LMXRBs (van Paradijs & White 1995). The presence of SXRTs in globular clusters is of particular interest, due to their possible evolutionary link with recycled MSPs. It is possible that some of the dim ($L_X \lesssim 10^{34}$ erg s $^{-1}$) X-ray sources in globular clusters are SXRTs in quiescence (e.g. Verbunt et al. 1994a; for an alternative explanation see e.g. Grindlay 1994).

In Table I we summarise the main properties of the presently known or suspected SXRTs. In the following we give a brief outline of the best studied objects. In the compilation of Table I we have included all the transients for which there are indications that they consist of a neutron star with a low mass companion, excluding ultrasoft X-ray transients which likely harbor a black hole. Sources which are sometimes defined as transients in the literature, but for which there is no clear evidence of flux variations greater than a factor of a ~ 100 , have not been included. Among these are: KS 1732–273, EU 1737–132, EXS 1737.9–2952, GRS 1741.9–2853, GS 1826–24.

2.1. Soft X-ray Transients with fast rise and exponential decay outbursts

2.1.1. Aql X-1

Aql X-1 (4U 1908+005) is the most active SXRT known: more than 30 X-ray and/or optical outbursts have been detected. This led to several attempts to correlate the properties of different outburst and to look for possible (quasi-)periodicities in the recurrence times. There is evidence that the peak intensity of an outburst correlates with the elapsed time from the previous one (White, Kaluziński & Swank 1984; Kitamoto et al. 1993). A recurrence time of ~ 125 d was quite evident in the 1969–1979 observations from the Ariel V and Vela 5B satellites (Priedhorsky & Terrell 1984). However, this periodicity did not

Table I: Minimum and quiescent luminosities of soft X-ray transients (with at least a few observations).

| Source | Other names | Distance (kpc) ^a | $\text{Log}_{10} L_{\text{min}}^{\text{obs}}$ during outburst (ergs^{-1}) ^b | Log_{10} Quiescent Luminosity (ergs^{-1}) | Outburst date(s) | P_{orb} (hr) | Comments ^c | Refs. ^d |
|------------------|---------------|-----------------------------|---|---|-------------------|-----------------------|-----------------------|--------------------|
| 3U 0042+32 | 2A 0042+323 | 10 | ~ 36.3 | | 1970 & 1977 | 278 (?) | O (?) | 1 |
| MX 0656-07 | | 10 | ~ 36 | | 1975 | | | |
| EXO 0748-676 | UY Vol | 10 | 36.6 | ~ 34 (0.5-10 keV) | from 1985 | 3.8 | B - O | 2, 3 |
| MX 0836-42 | | 10 | 36.5 | 35 (1-2.4 keV) | 1971/72 & 1990/91 | | B | 4 |
| Cen X-4 | V822 Cen | 1.5 | 35.5 | 32.5 (0.5-10 keV) | 1969 & 1979 | 15.1 | B - O | 5 |
| 4U 1608-522 | QX Nor | 3.5 | 36 | 33.3 (0.5-10 keV) | Recurrent | | B - O - Q | 5, 6 |
| 4U 1658-298 | V2134 Oph | 10 | ~ 36 | | 1978 | 7.2 | B - O | 7 |
| 4U 1730-335 | Rapid Burster | 10 | ~ 37 | 33.3 (0.5-10 keV) | Recurrent | | B | 8 |
| 4U 1730-22 | | 10 | 36.5 | | 1972 | | | 2 |
| KS 1730-312 | | 10 | ~ 37 | | 1994 | | | 9 |
| KS 1731-260 | | 8.5 | ~ 37 | | Sporadic | | B - Q | 10 |
| 4U 1735-28 | GX359+2 | 10 | 36.5 | | 1971 | | | |
| KS 1741-293 | MX 1743-29 | 10 | ~ 37 | | 1971 | | B | |
| A 1742-289 | | 8.5 | ~ 36 | ~ 35 (3-10 keV) | 1975 | 8.4 | B | 11 |
| 1743-288 | GX +0.2,-0.2 | 10 | ~ 37 | | 1971 & 1976 | | | 12 |
| A 1745-36 | | 10 | 36.3 | | 1976 | | | |
| MX 1746-20 | (NGC 6440) | 7 | 37.3 | 33.3 (0.5-4.5 keV) | 1971 | | | |
| EXO 1747-214 | | 10 | 35.6 | | 1985 | | B | 13 |
| GRS 1747-312 | (Ter 6) | 13 | 36.5 | | 1990? | | | 14 |
| 1749-285 | GX +1.1,-1.0 | 10 | ~ 37 | | 1976 | | | 12 |
| MX 1803-245 | | 10 | 37.3 | | 1976 | | | |
| SAX J1808.4-3658 | | ~ 4 | ~ 36.3 | | 1997 | | B | 15 |
| 1835-33 | (NGC 6652) | 14 | 35.9 | | 1990? | | | 14 |
| Aql X-1 | V 1333 Aql | 2.5 | 36.0 | 32.8 (0.5-10 keV) | Recurrent | 18.9 | B - O - Q | 16 |
| 4U 1918+15 | | 10 | ~ 36 | | 1972 | | | |
| 4U 2129+470 | V1727 Cyg | 6 | 36.8 | 32.8 (0.5-10 keV) | on up to 1981 | 5.2 | B - O | 2 |

^a When the distance was unknown a fiducial value of 10 kpc has been assumed.

^b Energy range 2 - 10 keV.

^c The label B indicates SXRTs where X-ray bursts have been detected; O indicates optically identified SXRTs and Q sources with kHz QPOs.

^d Data were mainly taken from van Paradijs (1995), Bradt & McClintock (1983) and Cominsky et al. (1978); additional references for particular sources have been quoted (see the bibliography to check out the numbers).

References: (1) Watson & Ricketts 1978; (2) Parmar et al. 1986; (3) Garcia & Callanan 1997; (4) Aoki et al. 1992; (5) Asai et al. 1996a; (6) Lochner & Roussel-Duprè 1994; (7) Cominsky & Wood 1984; (8) Asai et al. 1996b; (9) Trudolyubov et al. 1996; (10) Barret et al. 1992; (11) Maeda et al 1996; (12) Proctor et al. 1978; (13) Warwick et al. 1988; (14) Predehl et al. 1991; (15) in't Zand et al. 1998; (16) Campana et al. 1998.

extend to the time of more recent Ginga and optical observations (1987–1992), which on the contrary suggest of a ~ 310 d periodicity (Kitamoto et al. 1993). The outbursts of Aql X-1 are generally characterised by a fast rise (5–10 d) followed by a slow exponential decay, with an e -folding time of 30–70 d. Type I X-ray bursts were first discovered by Koyama et al. (1981) during the declining phase of an outburst. A periodicity of 132 ms, which persisted for only ~ 1 min, was detected during the peak of a type I burst observed with the Einstein SSS (Schoelkopf & Kelley 1991).

For a distance of $d \sim 2.5$ kpc, the corresponding 1–10 keV luminosity is $L_X \sim (0.9-4) \times 10^{37}$ erg s $^{-1}$. Close to the outburst maxima the X-ray spectrum is soft with $kT_{\text{br}} \sim 4-5$ keV. X-ray observations of Aql X-1 during the decay of an outburst have been collected in the $L_X \sim 10^{34} - 10^{36}$ erg s $^{-1}$ luminosity range. During the 1979 outburst Einstein MPC observed several times Aql X-1 (Czerny, Czerny & Grindlay 1987). The 1.2–10 keV spectrum when the source was at a level of a few 10^{36} erg s $^{-1}$ is well fit by a thermal bremsstrahlung model with the same temperature as in outburst. At a level of $\sim 10^{35}$ erg s $^{-1}$ the spectrum cannot be fit with the same model, but is instead consistent with a power-law model with photon index $\Gamma \sim 2.3$. The same power-law spectrum was recovered about half a year later when the source was at a level $\sim 2 \times 10^{34}$ erg s $^{-1}$ (Czerny, Czerny & Grindlay 1987). The ROSAT PSPC spectra during the 1990 and 1992 outbursts when $L_X \sim 10^{35} - 10^{36}$ erg s $^{-1}$ (0.1–2.4 keV) could not be fit satisfactorily by single component models (Verbunt et al. 1994b). Finally the ASCA spectrum (0.5–10 keV) when the Aql X-1 luminosity was $\sim 2 \times 10^{35}$ erg s $^{-1}$ was well fit by a single power-law with photon index $\Gamma \sim 2$ (Tanaka & Shibazaki 1996; Tanaka 1994). Moreover, several episodes of hard X-ray emission have been discovered by BATSE during 1991–1994 (Harmon et al. 1996), when the X-ray luminosity was about $\sim 4 \times 10^{36}$ erg s $^{-1}$. The X-ray spectra were characterised by a power-law of $\Gamma \sim 2-3$ and extending up to 100 keV.

Probably due to its closeness, Aql X-1 is one of a few SXRTs detected in quiescence. The ROSAT HRI and PSPC revealed Aql X-1 on three occasions at a level of $\sim 10^{33}$ erg s $^{-1}$ in the 0.4–2.4 keV range. During these observations the spectrum was very soft and could be well fit either with a black body model with a temperature of $kT_{\text{bb}} \sim 0.3$ keV, a thermal bremsstrahlung with a temperature of $kT_{\text{br}} \sim 0.8$ keV or a power-law with $\Gamma \sim 3$. The derived black body temperature implies an emitting radius of $\sim 10^5$ cm (Verbunt et al. 1994b).

An outburst from Aql X-1 reaching a peak luminosity of $\sim 10^{37}$ erg s $^{-1}$ (2–10 keV) was discovered (Levine et al. 1997) and monitored starting from mid-February, 1997 with the RossiXTE All Sky Monitor (see Fig. 1). Several pointed observations were successively carried out leading to the discovery of a nearly coherent modulation at ~ 550 Hz during a type I X-ray burst and a single QPO peak, with a frequency ranging from $\nu_{\text{QPO}} \sim 750$ to 830 Hz, at two different luminosities of $1.2 - 1.7 \times 10^{36}$ erg s $^{-1}$ (Zhang et al. 1998).

Observations carried out with the BeppoSAX Narrow Field Instruments (NFIs) starting from March 8th, 1997, allowed to study the final stages of the outburst decay (see Fig. 1; Campana et al. 1998). At the time of the first BeppoSAX observation (which started on March 8th, 1997) the source luminosity was decreasing very rapidly, fading by about 30% in 11 hr, from a maximum level of $\sim 10^{35}$ erg s $^{-1}$. The second observation took place on March 12th, 1997 when the source, a factor

of ~ 50 fainter on average, reduced its flux by about 25% in 12 hr. In the subsequent four observations the source luminosity attained its constant value of $\sim 6 \times 10^{32}$ erg s $^{-1}$ (0.5–10 keV). The sharp decrease after March 5th 1997 is well described by an exponential decay with an e -folding time ~ 1.2 d (see Fig. 1). The quiescent luminosity is consistent with the value previously measured with other satellites (e.g. Verbunt et al. 1994b).

The X-ray spectra during the fast decay phase, as well as that obtained by summing up all the observations pertaining to quiescence, could be fit with a model consisting of a black body plus a power-law. The soft black body component remained nearly constant in temperature ($kT_{\text{bb}} \sim 0.3-0.4$ keV), but its radius decreased by a factor of ~ 3 from the decay phase to quiescence. The equivalent radius in quiescence ($R_{\text{bb}} \sim 10^5$ cm) was consistent with the ROSAT results. The power-law component changed substantially from the decay phase to quiescence: during the decay the photon index was $\Gamma \sim 2$, while in quiescence it hardened to $\Gamma \sim 1$.

The optical counterpart of Aql X-1 was identified in 1978 with the variable K1IV star V1333 Aql (Thorstensen, Charles & Bowyer 1978; Shahbaz et al. 1996, 1997). Its quiescence magnitude is $V=19.2$ mag. Brightenings of up to ~ 5 mag have been observed during the X-ray outbursts. Chevalier and Ilovaisky (1991, 1997) monitored different optical outbursts of the source and determined a photometric orbital period of 18.9 hr.

Aql X-1 was observed at radio wavelengths with the VLA at 0.4 mJy (at 8.4 GHz) during an outburst (Hjellming et al. 1990). This source was also searched during the quiescent phase for pulsed radio emission at 400 MHz with the Jodrell Bank telescope. This provided an upper limit of ~ 10 mJy during June 1989 (Biggs, Lyne & Johnston 1989) and ~ 3 mJy during July–August 1989 (Biggs & Lyne 1996).

2.1.2. Cen X-4

Only two X-ray outbursts have been detected from Cen X-4. The second outburst was observed in 1979, ten years after the first one (Conner, Evans & Belian 1969). Their rise times were $\sim 5-7$ d and e -folding decay times of ~ 30 d. During the 1979 outburst Cen X-4 reached a peak flux of ~ 5 Crab, corresponding to $L_X \sim 4 \times 10^{37}$ erg s $^{-1}$ for $d \sim 1.2$ kpc (Kaluzienski, Holt & Swank 1980). Type I bursts were observed at intermediate luminosity levels (Matsuoka et al. 1980). A variable, hard spectral component extending up to ~ 100 keV and with an equivalent bremsstrahlung temperature kT_{br} of 30–70 keV was also revealed. This component appeared slightly before the outburst maximum, with a flux similar to that in the 3–6 keV range, and during the decay phase, with a factor of ~ 5 lower flux than the 3–6 keV flux (around $L_X \sim 2 \times 10^{37}$ erg s $^{-1}$; Bouchacourt et al. 1984). The 1979 outburst was particularly well studied and led to the identification of the optical counterpart which had brightened by $\gtrsim 6$ magnitudes (Canizares, McClintock & Grindlay 1979).

ASCA detected Cen X-4 during quiescence at a level of 2.4×10^{32} erg s $^{-1}$ (0.5–10 keV; Asai et al. 1996a). The X-ray spectrum was well fit by a black body component ($kT_{\text{bb}} = 0.16$ keV) plus an additional power-law component with $\Gamma \sim 2-3$. The flux from the two spectral components is comparable. The equivalent radius of the black body emission is $\sim 1.8 \times 10^5$ cm, substantially smaller than the radius of a neutron star. A search for X-ray pulsations gave negative results, providing

Aql X-1
Light Curve of Feb. 1997 outburst

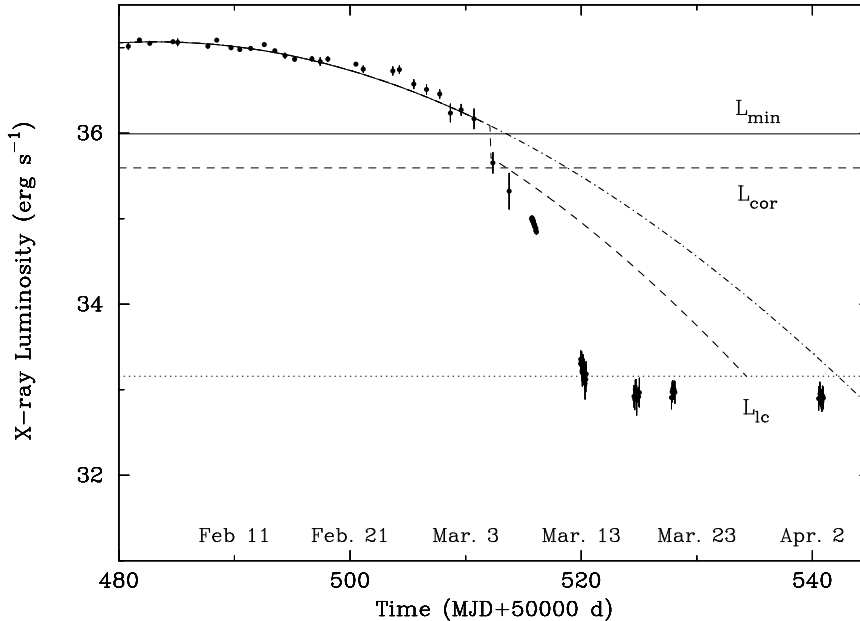


Fig. 1. Light curve of the Feb.-Mar. 1997 outburst of Aql X-1. Data before and after MJD 50514 were collected with the RossiXTE ASM (2–10 keV) and the BeppoSAX MECS (1.5–10 keV), respectively. RossiXTE ASM count rates are converted to (unabsorbed) luminosities using a conversion factor of $4 \times 10^{35} \text{ erg s}^{-1}$ (before MJD 50512) and $2 \times 10^{35} \text{ erg s}^{-1}$ (after MJD 50512) as derived from RossiXTE spectral fits (Zhang, Yu & Zhang 1998). BeppoSAX luminosities are derived directly from the spectral data (Campana et al. 1998). The evolution of the flux from MJD 50480 to MJD 50512 is well fit by a Gaussian centered on MJD 50483.2. This fit however does not provide an acceptable description for later times (see the dot-dashed line), not even if the accretion luminosity is calculated in the propeller regime (dashed line). The straight solid line represents the X-ray luminosity corresponding to the closure of the centrifugal barrier L_{\min} (for a magnetic field of 10^8 G and a spin period of 1.8 ms) and the straight dashed line the luminosity gap due to the action of the centrifugal barrier, L_{cor} . The dotted line marks the minimum luminosity in the propeller regime (L_{ic}).

an upper limit to the pulsed fraction of $\sim 50\%$ between 8 ms and 8200 s (Asai et al. 1996a). During quiescence Cen X-4 was also observed with the Einstein IPC (in 1980, $\sim 440 \text{ d}$ after the 1979 outburst; Petro et al. 1981) and EXOSAT CMA (in 1986, van Paradijs et al. 1987). Assuming the ASCA spectrum, Campana et al. (1997) found that both measurements are consistent with the same value of the X-ray luminosity derived with ASCA. A Ginga observation in 1991 provided an upper limit of $\sim 5 \times 10^{32} \text{ erg s}^{-1}$ in the range 2–7 keV (for a thermal bremsstrahlung spectrum with $T = 5 \text{ keV}$; Kulkarni et al. 1992). A ROSAT HRI observation in 1995 revealed Cen X-4 at a level comparable to that measured by ASCA, but showed a factor of 3 flux variability in a few days (Campana et al. 1997).

Cen X-4 is one of the best studied SXRTs at optical wavelengths. Extensive spectroscopic and photometric measurements of the optical counterpart in quiescence ($V=18.7 \text{ mag}$) led to the determination of the orbital period (15.1 hr; Chevalier et al. 1989) and the mass function ($\sim 0.2 M_{\odot}$, converting to a neutron star mass between $0.5 - 2.1 M_{\odot}$; Shahbaz, Naylor & Charles 1993). The optical spectrum shows the characteristics of a late K main sequence star, contaminated by lines and continuum emission probably resulting from an accretion disk (see, e.g., Cowley et al. 1988; Chevalier et al. 1989). The exact nature and evolutionary state of the companion star, together with the mechanism responsible for the mass transfer are the subject of a long debate. The most likely scenarios involve ei-

ther a peculiar subgiant or a stripped giant, filling its Roche lobe, and viewed at low inclination (McClintock & Remillard 1990; Shahbaz, Naylor & Charles 1993).

Radio emission had been revealed a few days after the 1979 outburst at a level of $\sim 10 \text{ mJy}$ at both 1.5 and 4.8 GHz (Hjellming et al. 1988). The quiescent phase of Cen X-4 was observed in the radio band with the VLA, searching for pulsations and/or continuum emission. Radio emission was not detected with an upper limit of 0.4 mJy at 1.4 GHz (Kulkarni et al. 1992).

2.1.3. 4U 1730–22

The only known outburst from this source was observed with Uhuru in 1972 (Forman et al. 1978). The decay of the X-ray flux was characterised by an e -folding time of $\sim 30 \text{ d}$ with evidence of a secondary maximum. The thermal bremsstrahlung-like spectrum, with a temperature of $\sim 4 \text{ keV}$, clearly indicated that this source belongs to the SXRT class (Cominsky et al. 1978).

2.1.4. A 1742–289

This SXRT, located close to the Galactic Center direction, underwent a strong outburst in 1975, characterised by a fast rise time to a peak flux of $\sim 2 \text{ Crab}$ (corresponding to a luminosity of $\sim 4 \times 10^{38} \text{ erg s}^{-1}$ at 8.5 kpc) followed by an exponential

decay with an e -folding time of 12 d (Branduardi et al. 1976). Though the source lies in a very crowded region, the concomitant radio outburst yielded an accurate position (Davis et al. 1976). ASCA has recently detected A 1742–289 at a 3–10 keV luminosity ranging between $10^{35} - 10^{36}$ erg s $^{-1}$ (Maeda et al. 1996). The source exhibited X-ray bursts and eclipses, yielding an orbital period of 8.4 hr. The X-ray spectrum is highly absorbed ($N_H \sim 10^{23}$ cm $^{-2}$) and could be well fit by a power-law with index 2.4 or a thermal bremsstrahlung model with $kT_{br} = 7.5$ keV. However, a reanalysis of the Ariel V data from the 1975 outburst provided no evidence for eclipses suggesting that the source detected by ASCA is perhaps a new one, rather than the quiescent counterpart of A 1742–289 (Kennea & Skinner 1996).

2.2. Soft X-ray Transients with extended on/off periods

The sources of this sample are characterised by on and off states lasting several months to years. Three out of four systems show partial X-ray eclipses and/or dips, indicating that they are viewed from a high inclination. In some instances there is strong evidence that the central X-ray source is hidden by the accretion disk and the observed X-rays are scattered along our line of sight by an extended photo-ionised corona above the disk (i.e. they are accretion disk corona sources; White & Holt 1982). A different case is presented by 4U 1608–52 which shows intermediate properties between this class of SXRTs and those displaying outbursts with fast rise and nearly exponential decay.

2.2.1. EXO 0748–676

EXO 0748–676 was discovered during a slew with the EXOSAT satellite in 1985. The intensity decayed in the first 2 months after the discovery, as expected for classical transients. However, in June–July 1985 and January 1986 it was again in a bright state with $L_X \sim 10^{37}$ erg s $^{-1}$ (Parmar et al. 1986). The source was still active when reobserved with Ginga in 1989 (Parmar et al. 1991) and more recently with ASCA, even if at a lower level (Corbet et al. 1994; Thomas et al. 1997). Type I bursts (with photospheric radius expansion), dips and partial eclipses at the 3.8 hr orbital period were observed with EXOSAT. Parmar et al. (1986) found a quiescent X-ray luminosity of 10^{34} erg s $^{-1}$ (0.5–10 keV), while Garcia & Callanan (1998) infer from the same data a black body temperature of $kT_{bb} \sim 0.2$ keV. Based on ASCA data Thomas et al. (1997) find evidence of a previously unreported soft excess. Optical observations, which detected EXO 0748–676 in the range $V \sim 17.5 - 16.8$ mag also testify that the source remained active during the period 1985–1993. Optical variability as well as optical bursts resulting from reprocessed X-ray bursts have also been observed.

2.2.2. 4U 2129+47

4U 2129+47 shows partial X-ray eclipses at the orbital period of 5.2 hours, as well as type I bursts. Before 1984 it was considered a persistent LMXRB, since it had been detected and studied with all the major X-ray satellites. Its relatively low luminosity and smooth orbital modulation at 5.2 hr in the active state ($\sim 10^{35} - 10^{36}$ erg s $^{-1}$ for $d \sim 6$ kpc) suggests that 4U 2129+47 is an accretion disk corona source (White & Holt 1982). During this active state the optical counterpart

was identified (Thorstensen et al. 1979). EXOSAT CMA observations in September 1983 provided only upper limits corresponding to a luminosity of $\lesssim 10^{34}$ erg s $^{-1}$ (Pietsch et al. 1986). Subsequent X-ray and optical observations showed that the source entered a long period of quiescence (Garcia et al. 1989; Molnar & Neely 1992) and led to its inclusion in the SXRT group. A ROSAT HRI observation detected this source at a level of $\sim 3 \times 10^{33}$ erg s $^{-1}$ (0.3–2.4 keV; Garcia 1994). Garcia & Callanan (1998) derived a quiescent luminosity of 6×10^{32} erg s $^{-1}$ (0.5–10 keV) for a black body spectrum with a temperature $kT_{bb} = 0.2$ keV. The quiescent X-ray light curve, obtained with the ROSAT HRI, does not show strong evidence for the partial eclipses characteristic of the active state, indicating that either the vertical extent of the disk is drastically reduced or that the disk is not present during quiescence (Garcia 1994). Note that the optical spectrum of 4U 2129+47 during quiescence does not display any characteristic feature of an accretion disk (Garcia 1994).

The companion was classified as a F9 subgiant, but no evidence was found of the expected ellipsoidal and radial velocity variations at the orbital period (Garcia et al. 1989).

An upper limit of ~ 8 mJy at 610 MHz for pulsed radio emission has been set for 4U 2129+47 during quiescence (Biggs, Lyne & Johnston 1989) and of 2 mJy at 400 MHz (Biggs & Lyne 1996); at 1.4 GHz the 4σ upper limit is of 0.25 mJy (Kulkarni et al. 1992).

2.2.3. 4U 1658–298

4U 1658–298, was discovered in 1976 when an isolated Type I burst was detected (Lewin, Hoffman & Doty 1976a). The corresponding SXRT was discovered only two years later during a strong outburst reaching a flux of $\sim 10^{-9}$ erg s $^{-1}$ cm $^{-2}$ (Lewin et al. 1978; Share et al. 1978). During this outburst, X-ray eclipses and dips were also detected (Cominsky, Ossmann & Lewin 1983). Hard X-rays up to ~ 80 keV from this source were revealed with the A4 experiment on board HEAO-1 (Levine et al. 1984).

2.2.4. 4U 1608–52

The persistent source 4U 1608–52 detected by Uhuru and OSO-7 in 1971–1973, and the transient observed with Ariel V in November 1975 and with Ariel V, SAS-3 and HEAO 1 in July–September 1977 were recognised to be the same object (Fabbiano et al. 1978 and references therein). The type I bursts (with photospheric radius expansion indicating a 3.6 kpc distance) observed from this region in the Norma constellation were also attributed to this source, thus providing the first case of transient-burster association. The bursts from 4U 1608–52 were later confirmed with HAKUCHO (Murakami et al. 1980) and EXOSAT (Penninx et al. 1989).

The Vela 5B data detected 8 outbursts during 1969–1979 as well as a persistent emission at a level of $\sim 10^{36}$ erg s $^{-1}$ (Lochner & Roussel-Duprè 1994). The outbursts are characterised by either a sharp rise and an exponential decay or a much more symmetric evolution. Like other SXRTs, 4U 1608–52 exhibited a spectral transition from a thermal bremsstrahlung to a power-law like spectrum when the luminosity decreased below $\sim 10^{37}$ erg s $^{-1}$ (Mitsuda et al. 1989). A hard power-law like spectrum has also been detected with BATSE during the 1991 outburst with a power-law slope of $\Gamma \sim 1.8$ and a steepening above ~ 65 keV (Zhang et al. 1996b).

The high energy spectrum could be equally well fit by either a Sunyaev-Titarchuk Comptonisation model or a broken power-law.

In 1993 ASCA revealed 4U 1608–52 at a much lower X-ray luminosity of $\sim 2 \times 10^{33}$ erg s⁻¹ in the 0.5–10 keV energy range (Asai et al. 1996a). The spectrum could be well fit by a black body with $kT_{\text{bb}} = 0.30$ keV or a bremsstrahlung with $kT_{\text{br}} = 0.32$ keV. The black body emission radius is $\sim 1.5 \times 10^5$ cm, substantially smaller than the radius of a neutron star. A periodicity search based on the ASCA light curves provided an upper limit of 50% rms in the range 8 ms–8200 s, which is valid only if the orbital period is longer than 2 d (Asai et al. 1996a).

This source was active again in 1996 and was observed by RossiXTE at a level of $\sim 2 \times 10^{37}$ erg s⁻¹ with a $kT_{\text{br}} \sim 5$ keV bremsstrahlung spectrum (Marshall & Angelini 1996). RossiXTE observations revealed also a variable QPO feature at 850–890 Hz, the frequency variations of which did not correlate with intensity changes (Berger et al. 1996). A second kHz QPO has been recently revealed at about 1100 Hz simultaneous with the 600–900 Hz peak (Yu et al. 1997) previously known (Mendez et al. 1998). There is evidence that the frequency separation varied between 230–290 Hz, perhaps providing the first example of a variable kHz peak separation in an atoll source.

The optical counterpart, identified during the 1977 outburst, is a reddened faint star ($I \sim 18.2$ mag) which becomes fainter in quiescence ($I > 20$ mag, $B > 22$ mag; Grindlay & Liller 1978). This was re-discovered during the 1996 outburst about 150 d after the peak at a level of $R = 20.2$ mag and $J = 17.2$ mag, when the source was still active in the X-rays (Wachter 1997). One year before the outburst the source was detected at $J = 18.0$ mag and $R > 22$ mag (Wachter 1997).

2.2.5. 4U 1730–335: the Rapid Burster

The Rapid Burster alternates periods of activity lasting several weeks, to period of quiescence, during which the X-ray luminosity decreases by more than three orders of magnitude. During the active periods the Rapid Burster emits a variety of combinations of type I and II bursts, making it unique among LMXRBs (Lewin et al. 1976b). Here we do not describe in detail the very complex phenomenology of this source and we refer to the review by Lewin, van Paradijs & Taam (1995) and references therein.

In the state in which the Rapid Burster shows the closest resemblance to other SXRTs, namely persistent X-ray emission and type I X-ray bursts, the average luminosity is about 10^{37} erg s⁻¹ (for the ~ 10 kpc distance of the globular cluster Liller 1) and the spectrum can be described by a thermal bremsstrahlung with $kT_{\text{br}} \sim 10$ keV (Barr et al. 1987). During quiescence an upper limit of $\sim 10^{34}$ erg s⁻¹ was obtained with Einstein (Grindlay 1981). Recently, the Rapid Burster has been detected in quiescence by ASCA at a level of 3×10^{33} erg s⁻¹ (Asai et al. 1996b). However, the ASCA point spread function ($\sim 3'$) is comparable to angular radius of the Liller 1 cluster ($3.3'$) and it cannot be ruled out that the measured X-ray flux is due to other sources within the cluster.

RossiXTE observations of X-ray bursts from the Rapid Burster did not lead to the discovery of kHz QPOs (Guerriero, Lewin & Kommers 1997). A radio transient with flux density correlated with the RossiXTE ASM X-ray flux of the Rapid Burster has been recently observed (Rutledge et al. 1998).

2.3. Soft X-ray Transients with poorly sampled outburst light curves

2.3.1. MX 0836–42

This source was discovered at the end of 1971 with OSO-7 and Uhuru (Markert et al. 1977; Cominsky et al. 1978) at a level of 8×10^{-9} erg s⁻¹ cm⁻². The spectrum was soft, but owing to poor coverage the light curve of the outburst could not be determined accurately. MX 0836–42 remained undetected until a new period of activity occurred in 1990–1991. Ginga detected a variable X-ray flux from this source from the end of November 1990 until February 1991. ROSAT observed an active state at a level of $\sim 10^{-10}$ erg s⁻¹ cm⁻² (1.0–2.4 keV) around the middle of November 1990 during the all sky survey and re-observed it at a level ~ 15 times lower in May 1991. These observations led to the discovery of Type I bursts (Aoki et al. 1992) and a substantial reduction of its error box (Belloni et al. 1993), confirming the LMXRB nature of this source.

2.3.2. MX 1746–20

Little is known about this transient which has been unambiguously observed only in January 1972. It was discovered with the OSO-7 satellite (Markert et al. 1975) and tentatively identified with the globular cluster NGC 6440. This association was also supported by the more precise source location obtained with the Uhuru data (Forman, Jones & Tananbaum 1976). The peak X-ray luminosity was about 10^{37} erg s⁻¹ for the distance of this cluster ($d = 7$ kpc). Cominsky et al. (1978) classified MX 1746–20 as a soft transient, on the basis of a spectral fit yielding a thermal bremsstrahlung temperature of ~ 4 keV.

It is generally assumed that the dim source detected with the Einstein HRI at a level of $\sim 10^{33}$ erg s⁻¹ in the globular cluster NGC 6440 (Hertz & Grindlay 1983) is the quiescent counterpart of MX 1746–20. ROSAT HRI observations confirmed this detection at a similar level (Johnston, Verbunt & Hasinger 1995).

2.4. Galactic Center transients

Over the last few years several X-ray sources in the Galactic Center region have been discovered with Ginga, TTM, ART-P and SIGMA (e.g. in't Zand et al. 1989; Sunyaev et al. 1991). Little is known about these sources, owing the lack of optical identifications, poor temporal coverage and spectral information. The maximum X-ray luminosity observed from KS 1730–312, 4U 1735–28, EU 1737–132, GS 1741.1–2859 are of the order of $L_X \sim 10^{38}$ erg s⁻¹. On the other hand the highest detected luminosities of KS 1732–273, EXS 1737.9–2952, GRS 1741.9–2853 are considerably lower ($L_X \sim 10^{37}$ erg s⁻¹). Some other sources were only a factor of a few above the instruments' detection thresholds: among these are KS 1632–477, KS 1724–356, KS 1731–260, KS 1739–304, KS 1741–293. It is therefore unclear whether these sources are to be considered transient sources and, in particular, SXRTs.

2.4.1. KS 1731–260

The best studied of the latter sources, KS 1731–260, shows only modest X-ray luminosity variations, casting doubts on its inclusion in the SXRT class. The source was discovered by TTM on board MIR-KVANT (Sunyaev 1989) at a level of

$\sim 10^{37}$ erg s $^{-1}$ (2–27 keV) for a distance of 8.5 kpc. The spectrum was well fit by a bremsstrahlung spectrum with $kT_{\text{br}} \sim 6$ keV; X-ray bursts were also observed (Sunyaev et al. 1990). KS 1731–260 was also detected by ART-P, SIGMA (revealing a hard energy tail extending up to energies of ~ 40 keV; Barret et al. 1992) and during the ROSAT all-sky survey (see e.g. Smith, Morgan & Bradt 1997). RossiXTE revealed a fairly coherent signal during a ~ 2 s interval starting at the end of the contraction phase of an X-ray burst. These oscillations likely indicate the presence of neutron star spinning at 1.9 ms (Smith, Morgan & Bradt 1997). Moreover, two simultaneous QPO peaks around 900 and 1160 Hz have also been discovered with RossiXTE (Wijnands & van der Klis 1997), the difference frequency of which is consistent with half the frequency observed by Smith, Morgan & Bradt (1997), suggesting that the neutron star spin period is instead ~ 3.8 ms.

3. Outburst models

Models of SXRT outbursts closely parallel models of dwarf nova outbursts. One group of models involves accretion disk instabilities (Cannizzo 1993 and references therein; Huang & Wheeler 1989; Mineshige & Wheeler 1989; Cannizzo, Chen & Livio 1995) and the other instabilities in the mass transfer from the companion star (Osaki 1985; Hameury, King & Lasota 1986). For a recent review see Tanaka & Shibazaki (1996).

In both approaches, a compact star is continuously accreting from a disk fed by a companion star filling or almost filling its Roche lobe and transferring matter at relatively low rate in quiescence. In disk instability models, the accretion disk can become locally thermally and viscously unstable due to strong opacity variations caused by partial ionisation of hydrogen (Cannizzo 1993). The mechanism of mass transfer instability instead relies on the slow expansion of the superadiabatic convective layers of the companion star which is irradiated by hard ($E \gtrsim 10$ keV) X-rays, supposedly produced by low-level accretion onto the neutron star surface (Hameury, King & Lasota 1986). After the onset of accretion at a high rate, the high energy radiation is intercepted by the evolving accretion disk and the companion contracts again within a few weeks, leaving a disk fed at a low rate.

In a critical review Lasota (1995) pointed out the major problems of these two classes of models: disk instability models fail to reproduce the observed recurrence times, which are usually too short; mass transfer instability models require a quiescent hard X-ray luminosity at a level of $10^{34} - 10^{35}$ erg s $^{-1}$ and a subgiant or stripped giant companion in order to produce outburst recurrences in the observed range.

In the framework of disk instability model van Paradijs (1996) recently singled out the importance of X-ray heating of the accretion disk. Including these effects, the modified disk instability criterion leads to recurrence times in agreement with those of SXRT outbursts. This supports the idea that the disk instability models apply.

Independent of the specific accretion instability responsible for the transient behaviour (which of course might be different from those outlined above), we focus our attention on the properties of SXRTs in outburst and during quiescence, to explore the different accretion regimes and to constrain the physical parameters of the neutron stars.

4. Accretion and other regimes in Soft X-ray Transients

If the neutron stars of SXRTs possess a magnetic field of at least $10^8 - 10^9$ G, as suggested by the evolutionary connection with MSPs and by the magnetospheric interpretation of the kHz QPOs observed in several LMXRBs, then regimes ranging from accretion onto the magnetic polar caps to radio pulsar activity are potentially accessible. Depending on the spin period and magnetic field, transitions from one regime to another can in principle occur during the outburst cycle, as a consequence of drastic changes in the mass inflow rate.

When SXRTs are in outburst, the occurrence of type I bursts and kHz QPOs as well as the similarity of their properties (especially the X-ray spectrum) with those of persistent LMXRBs testify that accretion down to the neutron star surface takes place. Matter inflowing from the inner Lagrangian point will give rise to an accretion disk in the Roche lobe of the compact object, due to its high angular momentum. The presence of a disk during the outburst phase is also inferred from the enhancement of the optical luminosity, the non-thermal continuum spectra and the presence of weak emission lines, which strengthen during the decline, especially Balmer lines (van Paradijs & McClintock 1995).

If the neutron star is magnetic, the accretion disk cannot extend to radii smaller than the magnetospheric radius, r_m , where the pressure of the magnetic dipole field ($P_{\text{mag}} \propto \mu^2 r^{-6}$, with μ the magnetic dipole moment³ and r the distance from the neutron star) balances the pressure of the incoming matter. We consider here the simpler case of spherical accretion (see also Paper I) and refer to appendix A for a more detailed treatment based on the Ghosh & Lamb magnetically threaded-disk model (1979a; 1979b; 1992). The magnetospheric radius in the spherical free-fall approximation is given by:

$$\begin{aligned} r_m^{sp} &= \left(\frac{\mu^4}{2GM\dot{M}^2} \right)^{1/7} \\ &= 2 \times 10^7 \dot{M}_{15}^{-2/7} B_9^{4/7} M_{1.4}^{-1/7} R_6^{12/7} \text{ cm} \end{aligned} \quad (1)$$

where $\dot{M} = 10^{15} \dot{M}_{15}$ g s $^{-1}$ is the accretion rate, $B = 10^9 B_9$ G, $M = 1.4 M_{1.4} M_\odot$ and $R = 10^6 R_6$ cm are the neutron star magnetic field, mass and radius, respectively. The inflow of matter can proceed toward the neutron star only if several conditions are met. Within r_m matter is enforced to corotate with the neutron star magnetosphere. X-ray pulsations are likely to occur if a sizeable fraction of the material gets attached to the magnetic field lines and accretion takes place preferentially onto the magnetic polar caps. Accretion onto the neutron star surface gives rise to a luminosity of

$$L(R) = GM\dot{M}/R \quad (2)$$

The X-ray luminosity decay from the outburst peak takes place as a consequence of the decreasing accretion rate. Accretion onto the neutron star surface can continue as long as the centrifugal drag exerted by the corotating magnetosphere on the accreting material (in almost Keplerian rotation) is weaker than gravity (i.e. the ‘‘centrifugal barrier’’ is open, e.g. Illarionov & Sunyaev 1975; Stella, White & Rosner 1986). On the contrary, accretion onto the neutron star surface is inhibited

³In the following we use the magnetic dipole moment $\mu = BR^3/2$, where B is the neutron star magnetic field and R the neutron star radius.

when the magnetospheric radius becomes larger than the corotation radius, $r_{\text{cor}} = \left(\frac{GM P^2}{4\pi^2}\right)^{1/3}$ (where P is the neutron star spin period), since the drag exerted by the neutron star magnetic field becomes super-Keplerian. When this occurs the system enters the “propeller” phase (i.e. the centrifugal barrier closes). Due to the scaling of r_m with \dot{M} (the magnetospheric radius expands as the accretion rate decreases), there exists a minimum mass inflow rate, \dot{M}_{min} , below which the centrifugal barrier cannot be penetrated; this corresponds to an accretion luminosity of

$$L_{\text{min}}(R) = GM\dot{M}_{\text{min}}/R \quad (3)$$

In Fig. 2 we sketch the dependence of the accretion luminosity as a function of the inflow rate. In the case of spherical accretion this equation becomes:

$$L_{\text{min}}^{sp}(R) = 2 \times 10^{36} B_9^2 M_{1.4}^{-2/3} R_6^5 P_{-2}^{-7/3} \text{ erg s}^{-1} \quad (4)$$

where P_{-2} the spin period in 10^{-2} s (note that Eq. 1 in Paper I is incorrect for a factor of 2). In the case of the Ghosh & Lamb disk (see Eq. 15) this limiting luminosity is about a factor of ~ 10 lower than for spherical accretion for the same set of parameters and for a critical fastness parameter $\omega_c = 0.5$ (see Appendix A). This is due to the smaller neutron star magnetosphere in the Ghosh & Lamb disk case (a factor of ~ 3 , see Eq. 22).

Constraints on the neutron star spin period and magnetic field can be inferred for a SXRT by comparing the minimum luminosity $L_{\text{min}}(R)$ defined in Eq. 3 to the minimum observed X-ray luminosity L_{min}^{obs} at the end of an outburst, as long as one can be confident that this luminosity is still produced by accretion onto the neutron star surface. For a given source, the minimum observed X-ray luminosity produced by neutron star accretion defines a line in the usual magnetic field – spin period ($B - P$) diagram for radio pulsars: in order to accrete at the observed rate, a neutron star must possess a spin period and magnetic field such as to lie to the right of that line. These lines are similar to the usual spin-up line which is drawn for $L = L_{\text{Edd}} = 1.8 \times 10^{38} M_{1.4} \text{ erg s}^{-1}$. Lines of constant L_{min}^{sp} are shown in Fig. 3 for different luminosities.

Once the centrifugal barrier closes (i.e. when $r_m \gtrsim r_{\text{cor}}$) the source enters the propeller regime. The accretion flow is halted at the magnetospheric radius and an accretion luminosity of up to

$$L(r_m) = GM\dot{M}_{\text{min}}/r_m \quad (5)$$

is released (see Fig. 2). In the case of spherical accretion and just after the closure of the centrifugal barrier (i.e. for $r_m \sim r_{\text{cor}}$) this luminosity is

$$L(r_{\text{cor}}) = 2 \times 10^{35} B_9^2 M_{1.4}^{-1} P_{-2}^{-3} R_6^6 \text{ erg s}^{-1} \quad (6)$$

In the case of disk accretion an extra factor of 1/2 is present on the right hand side of Eq. 5, due to the fact that, in general, the disk matter at r_m is expected to retain the kinetic energy of its orbital motion (note that the magnetosphere rotates faster) and therefore only 1/2 of the gravitational energy is released. (For a Ghosh & Lamb disk this luminosity is a factor of ~ 25 lower for the same set of parameters, see Appendix A). This transition is expected to occur when the matter inflow rate decreases below \dot{M}_{min} in the decay phase of an X-ray transient outburst (Stella, White & Rosner 1986); correspondingly

a sharp decrease of the X-ray luminosity should be observed. Corbet (1996) has shown that the ratio of accretion luminosity before and after the closure of the centrifugal barrier, Δ , does not depend on the neutron star magnetic field nor on the accretion rate but only on its spin period (and radius):

$$\Delta = \frac{L_{\text{min}}(R)}{L(r_{\text{cor}})} = \left(\frac{GM P^2}{4\pi^2}\right)^{1/3} \frac{1}{R} \quad (7)$$

In the case of disk accretion an extra factor of 1/2 is present (see above).

Evidence for such a transition associated to the onset of the centrifugal barrier was revealed in two HXRTs containing an X-ray pulsar (V0332+53 with a spin period of 4.4 s, Stella, White & Rosner 1986 and 4U 0115+63 spinning at 3.6 s, Tamura et al. 1992). Due to their relatively long spin periods, these X-ray pulsars are expected to have $\Delta \sim 400$. The transition to the propeller regime has probably been observed during the outburst decay of the SXRT Aql X-1 (Zhang, Yu & Zhang 1998; Campana et al. 1998). Note that for short a neutron star spin period (2–4 ms as for the case of Aql X-1), the luminosity jump across the centrifugal barrier is expected to be much smaller (e.g. $\Delta = 3$ for $P \sim 3$ ms) and the accretion luminosity in the magnetospheric accretion regime correspondingly higher. The transition to the propeller regime might be more gradual than assumed, due e.g. to a fraction of the inflowing material penetrating the magnetosphere at high latitudes and therefore accreting onto the neutron star surface (Stella, White & Rosner 1986; Corbet 1996).

There are also uncertainties related to the extent of the luminosity jump associated with the onset of the centrifugal barrier. Additional contributions to the luminosity on both sides of the centrifugal barrier might derive from the coupling of the magnetic field lines to the disk matter. Priedhorsky (1986) pointed out that if the neutron star’s magnetic field couples with matter in the inner disk beyond the magnetospheric boundary, the rotational energy removed by spin-down torques from the neutron star can be released in the disk, increasing its luminosity. Even in the absence of such a magnetic coupling, the propeller regime is probably characterised by the transfer of angular momentum and energy from the neutron star rotation to the inflowing matter, due to the azimuthal asymmetry of the magnetospheric boundary. The neutron star can therefore work as a flywheel, storing rotational energy during the spin-up phases and releasing it in the disk during spin-down phases and likely also in the propeller regime. For fast rotating neutron stars these processes can lead to a substantially higher luminosity than that produced through accretion (see e.g. Priedhorsky 1986), therefore making the transition to the propeller regime more difficult to observe.

Despite all these uncertainties, the onset of the propeller regime in a SXRT might be revealed through a sudden spectral change or a steep decrease of the X-ray flux, as in the case of RossiXTE and BeppoSAX observations of Aql X-1 (Zhang, Yu & Zhang 1998; Campana et al. 1998).

In the propeller regime, matter accreting onto the magnetospheric boundary will in any case release its binding energy (see Eq. 5). In the case of spherical accretion this luminosity amounts to

$$L^{sp}(r_m) \sim 10^{34} B_9^{-4/7} M_{1.4}^{8/7} \dot{M}_{15}^{9/7} R_6^{-12/7} \text{ erg s}^{-1} \quad (8)$$

(In the case of disk accretion a luminosity by a factor of 2 lower should result). The luminosity in the disk accretion case is com-

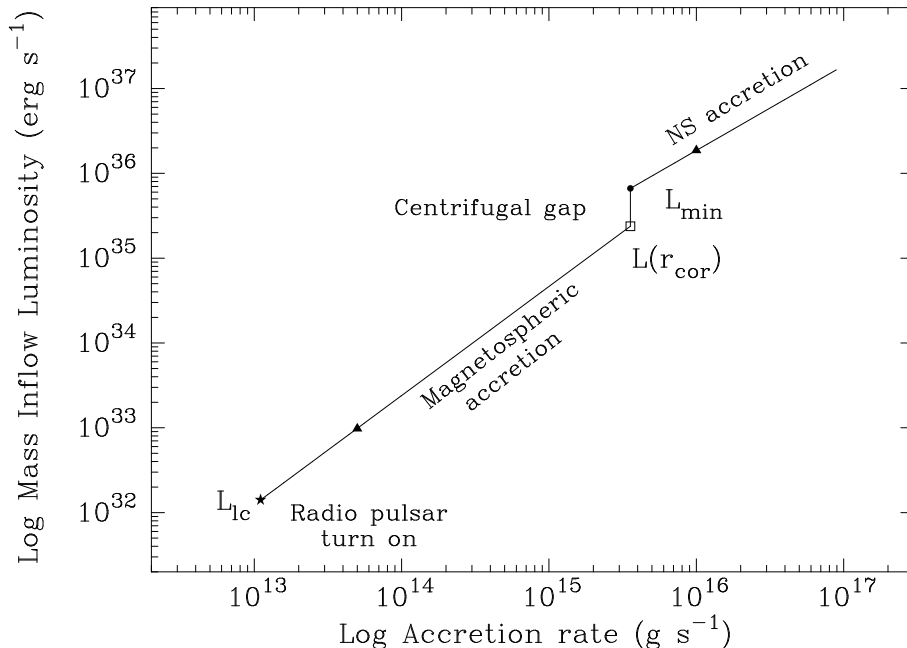


Fig. 2. Different regimes of spherical accretion onto a rotating magnetic neutron star for decreasing mass inflow rates (see arrows). A neutron star with spin period of 4 ms and magnetic field of 10^8 G has been considered. The upper line describes accretion onto the neutron star surface ($L_X \propto \dot{M}$, cf. Eq. 2). The filled dot represents the onset of the centrifugal barrier, corresponding to Eq. 3. The open square marks the point where the centrifugal barrier is closed and a much smaller luminosity is released from accretion onto the magnetosphere (cf. Eq. 5). In this regime the emitted luminosity is $L_X \propto \dot{M}^{9/7}$ (cf. Eq. 8). For even lower mass inflow rates the radio pulsar mechanism can turn on (filled star, see text and Eq. 9).

parable to that of the spherical case, due to the similar extent of the magnetosphere for the same accretion rate (cf. Eq. 22). In the propeller regime the fate of the infalling matter is uncertain: it can either be swept away by the magnetospheric drag at the expense of the rotational energy of the neutron star (as a result of either a supersonic or a subsonic propeller; Davies & Pringle 1981; Ghosh 1995) or accumulate outside the magnetospheric boundary possibly giving rise to a quasi-steady atmosphere (Davies & Pringle 1981). In the latter case, the accumulation of matter at the magnetospheric boundary can give rise to a pressure build-up, that might eventually push the magnetospheric boundary inside the corotation radius, therefore leading to accretion onto the neutron star surface.

The steep luminosity decline that characterises the propeller phase in Aql X-1 is considerably faster than what would be expected extrapolating the mass inflow rate from the first part of the outburst to the magnetospheric accretion regime (see Fig. 1). We note that the spectral transition accompanying the onset of the centrifugal barrier may modify the irradiation of the disk, therefore speeding up the end of the outburst (Campana et al. 1998). Alternatively, if matter ejection takes place in the propeller phase, its interaction with the inflowing matter can

contribute in turning off the outburst.

As the mass inflow rate decreases further, the magnetospheric radius expands until it reaches the light cylinder radius ($r_{lc} = cP/2\pi$, with c the speed of light). Consequently, the neutron star electromagnetic pressure thus changes from static ($\propto r^{-6}$) to radiative⁴ ($\propto r^{-2}$). The pressure of the inflowing material scales as $r^{-5/2}$ in the case of spherical symmetry; it can be shown that scales as r^α with $-7/2 < \alpha < -51/20$ for a standard accretion disk depending on the chosen region. The radiative pressure of the radio pulsar is therefore characterised by a flatter radial dependence than the pressure of the inflowing matter. If the pressures balance at r_{lc} , then for any larger radii the pulsar radiation pressure will dominate. Under these conditions, no stable equilibrium exists and the accreting matter begins to be pushed outwards (Illarionov & Sunyaev 1975; Shaham & Tavani 1991). Matter inflowing through the Roche lobe is stopped by the radio pulsar radiation pressure, giving

⁴The fraction of the radiation pressure interacting with matter has been estimated to be ~ 1 from studies of bow-shock nebulae around radio pulsars (Kulkarni & Hester 1988; Cordes, Romani & Lundgren 1993).

rise to a shock front.

The limiting mass inflow rate, \dot{M}_{lc} , below which the radio pulsar mechanism will turn on, is determined by the condition $r_m \sim r_{lc}$. This corresponds to a minimum luminosity produced by accretion onto the magnetosphere of

$$L_{lc} = L(r_{lc}) = G M \dot{M}_{lc} / r_{lc} \quad (9)$$

which in the spherical approximation becomes

$$L_{lc}^{sp} = 7 \times 10^{31} B_9^2 M_{1.4}^{1/2} P_{-2}^{-9/2} R_6^6 \text{ erg s}^{-1} \quad (10)$$

In the case of disk accretion a factor of ~ 70 lower luminosity is expected for the same set of parameters (see Eq. 17). The observability of a radio pulsar signal during this phase is discussed in detail in the Section 5.3.1. In this regime, a fraction of the neutron star spin-down luminosity can be emitted in the X-ray band as a result of the interaction between the relativistic pulsar wind and the incoming matter. A conversion efficiency of the spin-down luminosity up to $\sim 10\%$ can be expected in these systems (Tavani 1991; see also below).

The mass inflow rate required to overcome the pulsar radiation barrier is higher than that for which the radio pulsar turns on, such that a limit cycle is expected. In fact, in order to overcome the pulsar radiation, the pressure of the matter inflow must dominate the radiation pressure ($P_{rad} = L_{sd}/4\pi r c$, where L_{sd} is the spin-down luminosity) at the shock radius, in the proximity of the inner Lagrangian point (where matter spills out with almost constant pressure, dominated by its thermal energy, e.g. Meyer & Meyer-Hofmeister 1983). Once the radiation barrier is won, the matter inflow can proceed inside the light cylinder radius quenching the radio pulsar mechanism (e.g. Illarionov & Sunyaev 1975; Shaham & Tavani 1991; Lipunov 1992).

The condition for the quenching the radio pulsar emission is not easy to derive as it depends on the geometry of the shock front. The most likely possibility is represented by the formation of an ‘‘outer bubble’’, supported internally by pulsar radiation pressure and continuously fed by mass loss from the companion (as in the case of PSR 1744–24A; Lyne et al. 1990; Tavani & Brookshaw 1991, 1993). An accurate estimate of the mass needed to overcome the pulsar pressure requires detailed magneto-hydrodynamical simulations.

5. X-ray emission in quiescence

Several SXRTs have been detected during the quiescent phase at a level of $L^q \sim 10^{32} - 10^{33} \text{ erg s}^{-1}$. The X-ray spectra observed by ROSAT are usually soft and are characterised by a black body temperature of $\sim 0.3 \text{ keV}$ or, equivalently, a power-law slope of $\Gamma \sim 3$ (as detected in the 0.1–2.4 keV energy band). Observations with larger energy bands (ASCA, BeppoSAX) have provided evidence for the existence of a hard energy tail, in addition to the soft black body spectrum in Aql X-1 and Cen X-4 during their quiescence states.

The origin of this quiescent X-ray emission is still open to a number of possibilities. Coronal activity of the companion star can be ruled out since late type low mass stars produce an X-ray luminosity of $10^{32} \text{ erg s}^{-1}$ at the most (Dempsey et al. 1995; Verbunt 1996). The quiescent emission in SXRT could result from:

- (1) accretion onto the neutron star surface;
- (2) accretion down to the magnetospheric radius (when the ‘‘centrifugal barrier’’ is closed, Paper I);

- (3) non-thermal processes powered by the rotational energy loss of a rapidly spinning neutron star (Tavani & Arons 1997);
- (4) thermal emission from the cooling neutron star.

5.1. Accretion onto the neutron star surface

In this regime, the requirement that the centrifugal barrier is open for $L_{min}^{obs} = 10^{33} \text{ erg s}^{-1}$ translates into a fairly stringent condition on the neutron star parameters, implying long spin periods and/or low magnetic fields (see Eq. 4 and Fig. 3; Paper I; Verbunt 1996).

For the neutron star spin period frequency of 2–4 ms inferred from recent observations of Aql X-1, accretion onto the neutron star surface during quiescence can take place only if $\lesssim 5 \times 10^6 \text{ G}$. In this case then SXRTs could not be among the progenitors of MSPs.

Models of the X-ray emission produced by a weakly magnetic neutron star accreting (onto the polar caps) at $\sim 10^{33} \text{ erg s}^{-1}$ predict a soft black body spectrum ($kT_{bb} \sim 0.4 \text{ keV}$) with a (weak) high energy tail due to Compton heating of thermal photons in the external part of the hot atmosphere (Zel’dovich & Shakura 1969; Zampieri et al. 1995). Available X-ray spectra of the quiescent state of several SXRTs are consistent with a black body model with an emitting area a factor of $\sim 10^{-2}$ smaller than the neutron star surface, even if the recent evidence for a hard tail in both Cen X-4 and Aql X-1 cannot easily be accounted for by this model.

5.2. Accretion down to the magnetospheric radius

Another possibility is that the quiescent state of SXRTs is powered by accretion onto the magnetospheric boundary, such that an accretion luminosity of $L_m = G M \dot{M} / r_m$ is released (reduced by a factor of 2 in the likely case of disk accretion). This propeller regime is characterised by $r_{cor} \lesssim r_m \lesssim r_{lc}$ (see Eq. 9) and, therefore, the accretion luminosity released by the disk is $L_{lc} \lesssim L_{rm} \lesssim L_{cor}$. In Fig. 3, the lines of constant L_{lc}^{sp} and L_{cor}^{sp} are drawn. It should be emphasised that L_{rm} provides only a lower limit to the total quiescent luminosity, which might include additional contributions from the release of neutron star rotational energy through the interaction between the rotating magnetosphere and the inflowing matter. Assuming that most of the quiescent luminosity L^q of a SXRT results from accretion onto the magnetosphere, the neutron star is constrained to lie in the region of the $B - P$ diagram between the lines $L^q = L_{lc}$ and $L^q = L_{cor}$. For $L^q = 10^{33} \text{ erg s}^{-1}$, this region is fairly wide and contains a large number of MSPs (see Fig. 3), even though it is relatively distant from the classical spin-up line. In this interpretation, the neutron stars of SXRTs cannot be the progenitors of the highest magnetic field MSPs. Note that the line $L_{lc} = 10^{33} \text{ erg s}^{-1}$ straddles the region of the $B - P$ diagram where neutron stars of LMXRBs are expected to lie, according to the beat-frequency interpretation of the kHz QPOs.

Little theoretical work has been carried out so far on the spectrum emitted by a neutron star in the propeller regime. If the inflowing matter is in the form of an optically thick accretion disk, most of the flux should be emitted in the UV/soft X-ray band (e.g. Shakura & Sunyaev 1973). If the magnetosphere remains small (as expected for low magnetic fields and spin periods) a hot, inner Comptonising corona might form in analogy with the case of persistent LMXRBs, giving rise to a power-law like spectrum. One might speculate that the formation of an inner disk corona is due to the interaction between

Spherical accretion

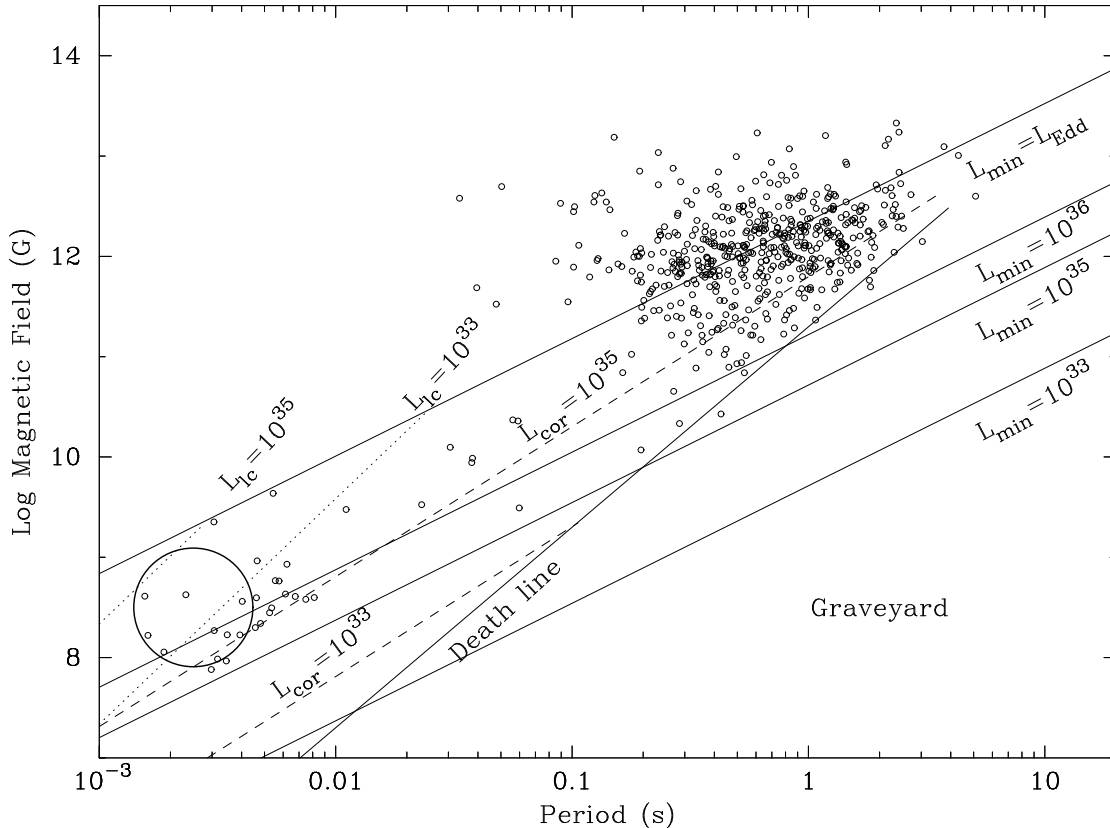


Fig. 3. Surface magnetic field plotted versus spin period of known pulsars (circles), taken from Taylor, Manchester & Lyne (1993). The death line corresponds to the polar cap voltage below which the radio pulsar activity switches off (e.g. Bhattacharya & van den Heuvel 1991). The death line is here described as $B_9 \simeq 2 \times 10^{-2} P_{-2}^2 R_6^{-3}$ G (Ruderman & Sutherland 1975; Bhattacharya & van den Heuvel 1991; Chen & Ruderman 1993). However, Rudak & Ritter (1994) and Phinney & Kulkarni (1994) suggested to reshape the death line in the MSPs region to account for curvature radiation reaction. This results in a flatter death line for spin periods smaller than ~ 0.1 s, nearly coincident with the locus of pulsars with characteristic age $\tau_c = P/(2\dot{P})$ equal to the age of the Universe (10 Gyr, i.e. the so-called “Hubble” line; here P is the spin period derivative). A different death line was suggested by Björnsson (1996). In this paper, however, we adopt the standard death line. For more details on the death line, the graveyard and the “Hubble” line see Srinivasan (1989). Solid lines represent the limit given by Eq. 4 (in erg s^{-1}). Note that the line for $L = L_{\text{Edd}} = 1.8 \times 10^{38} M_{1.4} \text{ erg s}^{-1}$ corresponds to the so called spin-up line. Lines marking the maximum accretion luminosity emitted in the propeller regime (i.e. for $r_m = r_{\text{cor}}$) are indicated with dashes for selected luminosities (in erg s^{-1} units). Lines corresponding to the minimum accretion luminosity in the propeller regime (i.e. for $r_m = r_{\text{lc}}$) are depicted for selected luminosities (measured in erg s^{-1}) with dots. Therefore, if a neutron star is in the propeller regime and produces a given accretion-induced luminosity, then it must lie within the region between the corresponding lines L_{cor} and L_{lc} . The large circle in the millisecond period-low magnetic field region includes the kHz QPO sources.

the disk and the magnetosphere in the propeller regime (e.g. through shocked plasma).

In the case of Aql X-1 the onset of the propeller is marked by a steep increase of the hardness ratio (Zhang, Yu & Zhang 1998). The BeppoSAX spectrum shows a soft component (modeled as a black body with $kT_{\text{bb}} \sim 0.3$ keV) together with a power-law with photon index ~ 2 extending up to ~ 100 keV (see Section 2.1.1 and Campana et al. 1998).

5.3. Pulsar shock emission

One can infer the magnitude of the X-ray emission that would be expected in the case of pulsar-driven SXRTs nebulae in quiescence, relying on the recent observations of the PSR B1259–63 system and the theory of plerionic high-energy emission. As

the observations of the binary MSP PSR B1259–63 demonstrate (Tavani & Arons 1997), non-thermal X-ray emission is produced by the interaction of the relativistic pulsar wind with gaseous material. ASCA (Kaspi et al. 1995) and Compton GRO (Grove et al. 1995) observations of the 47 ms pulsar PSR B1259–63 near periastron (when the pulsar interacts more strongly with the outflow from the Be star companion) clearly show a power-law spectrum with $\Gamma \sim 1.6 - 2.0$ extending from ~ 1 keV up to ~ 200 keV as well as absence of pulsations. The high-energy emission near periastron cannot be due to accretion onto the surface of the neutron star (Tavani & Arons 1997) nor to accretion down to the magnetospheric radius (Campana et al. 1996). Rather it is in agreement with a synchrotron model of plerionic-like high-energy shock emission expected for a pul-

sar wind composed of electrons, positrons and possibly ions constrained to have Lorentz factor $\gamma_1 \gtrsim 10^6$ and plasma magnetisation Σ (ratio of Poynting energy flux to the particle kinetic energy flux) less than unity. The PSR B1259–63 observed broad-band efficiency of conversion of pulsar spin-down energy into high-energy radiation is (in the energy range 1–200 keV) $\varepsilon_{1259-63} \sim 1-3\%$ (Kaspi et al. 1995; Grove et al. 1995). Emission of comparable efficiency is expected also to be radiated in that system between 200 keV and 1–5 MeV (Tavani & Arons 1997). The observed shock efficiency depends obviously on the geometric characteristics of the pulsar cavity containing the pulsar wind. Since the PSR B1259–63 pulsar wind pressure probably disrupts the equatorial Be star outflow by ‘breaking open’ the disk-like outflow, the overall efficiency may be lower than for a spherically symmetric pulsar cavity (as in the case of the Crab Nebula, e.g. Kennel & Coroniti 1984).

If the acceleration shock timescale is less than the cooling timescale, the high-energy emission has a non-thermal nature (cooling is caused by synchrotron emission and possibly inverse Compton scattering in the optical background from the companion star). In this case, the power-law energy spectrum, calculated in an acceleration model based on magnetosonic absorption of ion induced waves (e.g. Arons & Tavani 1993), falls in the range $\varepsilon_1 < \varepsilon < \varepsilon_m$, where $\varepsilon_1 = 0.3\gamma_1^2 \hbar \omega_{cyc}(B_2)$ (typically $\varepsilon_1 \sim 1$ eV for $B_9/P_{-2}^3 \sim 1$; \hbar is the rationalised Planck’s constant) with ω_{cyc} the electron/positron cyclotron frequency and

$$\varepsilon_m = \gamma_m^2 \hbar \omega_{cyc}(B_2) \simeq 35 \left(\frac{\eta}{0.3}\right)^2 v_8 \left[\frac{n_8}{(1+\Sigma)}\right]^{1/2} \left(\frac{\Sigma}{0.005}\right)^{1/2} \frac{B_9}{P_{-2}^3} \text{ keV} \quad (11)$$

is the emission energy for the upper exponential cutoff of the synchrotron spectrum. In Eq. 11 we use the notation $v_8 = v/(10^8 \text{ cm s}^{-1})$ for the outflow velocity at the shock radius distance, $n_8 = n/(10^8 \text{ cm}^{-3})$ for the nebular density and η for the efficiency of particle acceleration in the pulsar magnetosphere as defined in Arons & Tavani (1993). In Eq. 11 it is assumed that a (conservative) maximum-to-initial ratio of post-shock energies $\gamma_m/\gamma_1 \sim 10$. The power-law index depends on the shock acceleration injection mechanism and efficiency. Based on the analogy with the PSR B1259–63 system, we infer a photon spectral index $1.6 \lesssim \Gamma \lesssim 2$, for an index of the underlying post-shock energy distribution function of the radiating pairs in the range $\sim 2-3$.

Substantial flux in the hard X-ray range should be observable for the acceleration-dominated case especially in the case of fast spinning neutron stars, and the spectral shape might provide an interesting signature for the existence of enshrouded pulsars in SXRTs. In particular power-law spectra are predicted, the photon index of which can be related to the characteristics of the shock front between the radio pulsar and the incoming matter.

The luminosity budget of quiescent SXRTs can be accounted for by a radio pulsar only if it is spinning rapidly at a few millisecond level and has a magnetic field of at least 10^8 G. Fig. 4 shows the lines of constant spin-down luminosity in the $B-P$ diagram. Assuming a conversion efficiency of spin-down luminosity to X-ray of $\varepsilon \sim 1-10\%$, which is plausible for enshrouded pulsars (Tavani 1991), we can match the $\sim 10^{33} \text{ erg s}^{-1}$ luminosity observed in quiescent SXRTs, if their neutron stars lie in the region between $L_{sd} = 10^{34}$ and

$10^{35} \text{ erg s}^{-1}$. Note that the low B and P section of this region overlaps quite well with the region inferred from the beat-frequency interpretation of the kHz QPOs in LMXRBs.

For the pulsar shock emission regime to apply to the quiescent state of SXRTs, the transition to the propeller regime must take place at a relatively high luminosity. In particular, if the neutron star spin period is 2–4 ms and the magnetic field $\sim 10^8 - 10^9$ G (as indicated by kHz QPO sources), the transition to the propeller regime involves a small luminosity gap (a factor of a few; cf. Eq. 7) and is expected to take place at a luminosity level of $\sim 10^{35} - 10^{37} \text{ erg s}^{-1}$ (cf. Eq. 4).

The outburst decay of Aql X-1 as observed with RossiXTE and BeppoSAX showed a small jump in luminosity around $10^{36} \text{ erg s}^{-1}$ followed by a sudden increase in the hardness ratio and steepening of the luminosity decay. These phenomena likely indicate the onset of the centrifugal barrier (Zhang, Yu & Zhang 1998; Campana et al. 1998). The quiescent emission of Aql X-1 has been investigated in detail with BeppoSAX. The spectrum can be satisfactorily fitted by a soft black body component plus a hard power-law with photon index of $1-1.5$ (Campana et al. 1998). The quiescent spectrum is significantly different from the one observed after the closure of the centrifugal barrier (characterised by a power-law photon index of ~ 2), suggesting that another change in the powering mechanism occurred. The quiescent X-ray luminosity of $6 \times 10^{32} \text{ erg s}^{-1}$ is consistent with being powered by shock emission induced by the relativistic wind of the rapidly spinning neutron star. The required 0.1–10% conversion efficiency of spin-down luminosity to X-rays is consistent with modeling and observations of enshrouded pulsars (Tavani 1991; Verbunt et al. 1996).

We note also the the ASCA spectrum of Cen X-4 shows a power-law component extending up to at least ~ 5 keV in addition to a soft component with an equivalent black body temperature of ~ 0.3 keV and comparable luminosity (Asai et al. 1996a), suggesting that also in this case the shock emission mechanism could be at work.

5.3.1. Observability of pulsed radio emission in SXRTs

We address here the expected radio luminosity of the MSPs contained in SXRTs. Taking the empirical relation between the mean pulsed luminosity at 400 MHz radio pulsar magnetic field and spin period for MSPs (Kulkarni, Narayan & Romani 1990), we derive a radio luminosity of $L_{\text{radio}} \sim 40 B_9^{2/3} P_{-2}^{-4/3} \text{ mJy kpc}^{-2}$. The minimum detectable radio flux increases fairly rapidly for decreasing periods. Moreover, the dispersion measure will heavily limit the observations: the mean dispersion measure of MSPs is about 40 pc cm^{-3} , with only a few MSPs with a value higher than 100 pc cm^{-3} .

The visibility of pulsed radio emission is made more difficult also by the presence of the matter spilling out of the first Lagrangian point into the Roche lobe of the compact object. If an ‘outer bubble’ supported by pulsar radiation pressure ensues (as in the case of PSR 1744–24A; Lyne et al. 1990) radio pulsed signal could only be observed sporadically, if at all (Tavani 1991). Hydrodynamic simulations aimed at modeling the shock front and the evolution of the enshrouding matter (Brookshaw & Tavani 1995) indicate that only for small inclination angles pulsed radio emission can propagate relatively undisturbed. In particular, the optical depth to free-free (bremsstrahlung) absorption caused by the material outflowing from the companion star can easily be much larger than unity (Brookshaw & Ta-

Spherical accretion

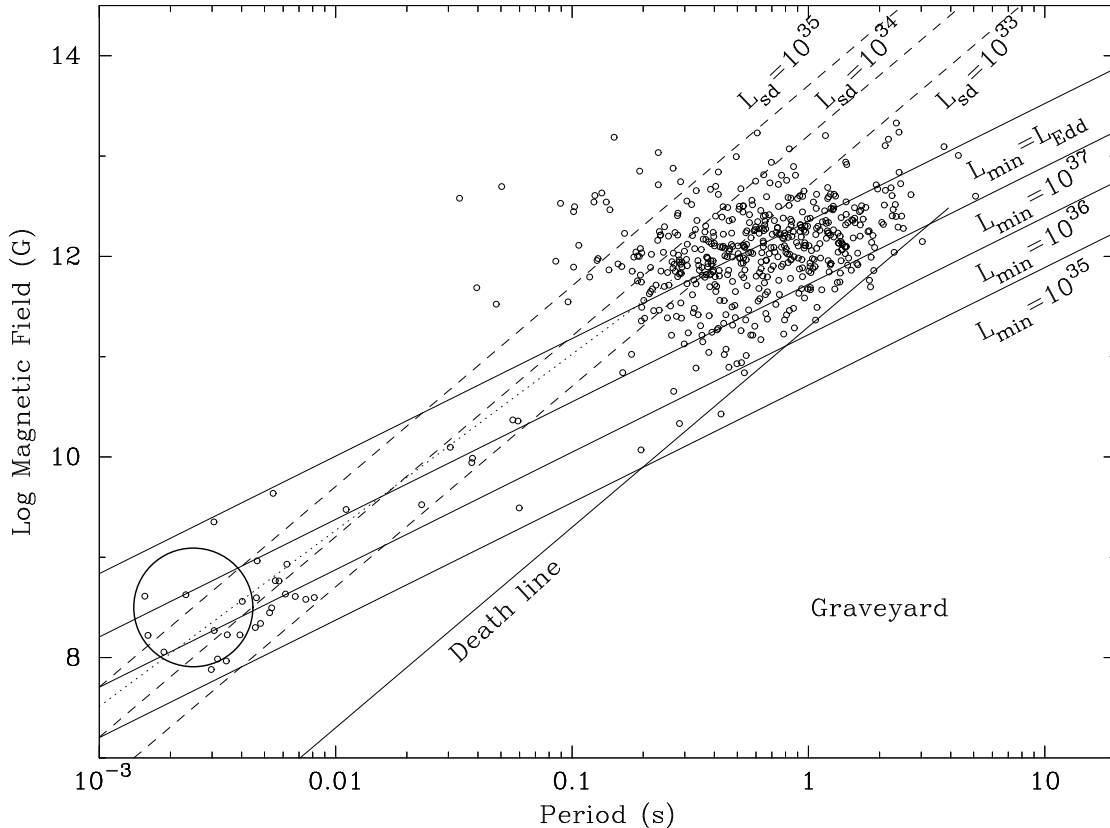


Fig. 4. Surface magnetic field plotted versus spin period of known pulsars (circles). The Eddington spin-up line is shown as a continuous line as well as other spin-up lines for selected luminosities. Dashed lines mark selected values of the spin-down luminosity. The dotted line separates the region in which the neutron star in a SXRT is expected to undergo secular spin-down (left) from that in which spin-up takes place (right) in the case of a radio pulsar being active during the quiescent phase (see also text). The large circle in the millisecond period-low magnetic field region includes the kHz QPO sources.

vani 1995). On the contrary, if radiation pressure sweeps away the mass inflow all together (as in the case of PSR 1957+20; Fruchter et al. 1992), the region between the two stars remains almost “clean”, providing favourable conditions for observing a MSP during the quiescent phase of a SXRT. We therefore conclude that radio observations of SXRTs in quiescence may not reveal any flux (continuum or pulsed) and still be compatible with the existence of an underlying enshrouded pulsar.

5.4. Black body emission from the neutron star surface

The quiescent X-ray flux could originate from the release of thermal energy at the surface of a moderately hot neutron star. The emission may result from radiative cooling of the warm interior heated up during the accretion episodes giving rise to the outbursts. This possibility is briefly investigated in Appendix B.

It is known that steady accretion at large enough accretion rates (i.e. $\dot{M} \gtrsim 3 \times 10^{14} \text{ g s}^{-1}$) causes the neutron star interior to increase its temperature owing to the release of energy by stable hydrogen burning ignited at the base of the envelope (Fujimoto et al. 1984; Miralda-Escudé, Paczyński & Haensel 1990). On a relatively short time scale of $t_{c,eq} \sim$

$2 \times 10^4 \dot{M}_{17}^{-3/4} \chi_{-3}^{-3/4} M_{1.4}^{3/4} \text{ yr}$ (where $\chi = \chi_{-3} 10^{-3}$ is the nuclear burning efficiency), the equilibrium between nuclear heating and neutrino cooling results in a core temperature $T_{c,8}^{eq} \sim 2.4 \times 10^8 \dot{M}_{17}^{1/8} \chi_{-3}^{1/8} M_{1.4}^{-1/8}$. Radiation from the warm interior released at the surface could then be revealed when accretion stops. Since a temperature gradient is established across the envelope, thermal radiation at a temperature of $T_s \sim 1.4 \times 10^6 \dot{M}_{17}^{1/12} \chi_{-3}^{1/12} M_{1.4}^{-1/12} \text{ K}$ is emitted, giving rise to a black body luminosity of $L_s \sim 3 \times 10^{33} R_6^2 \dot{M}_{17}^{1/3} \chi_{-3}^{1/3} M_{1.4}^{-1/3} \text{ erg s}^{-1}$ (Gudmundsson, Pethick & Epstein 1983).

This estimate provides only an *upper limit* since the (possible) presence of a pion condensate in the star’s interior reduces considerably the core temperature and, in turn, the temperature of the thermal radiation emitted at the stellar surface. In addition, owing to the intermittent character of accretion in a SXRT, the time necessary to attain equilibrium is $\sim t_{c,eq} \times \Theta$ (where Θ is the ratio of the recurrence time to the duration time of a SXRT outburst); this time can exceed the time over which heat leaks out through the envelope. This would further reduce the upper limit on $T_{c,8}^{eq}$ and in turn the black body luminosity L_s observed in quiescence. In Fig. 5, L_s is plotted against the mean accretion rate during outburst, for differ-

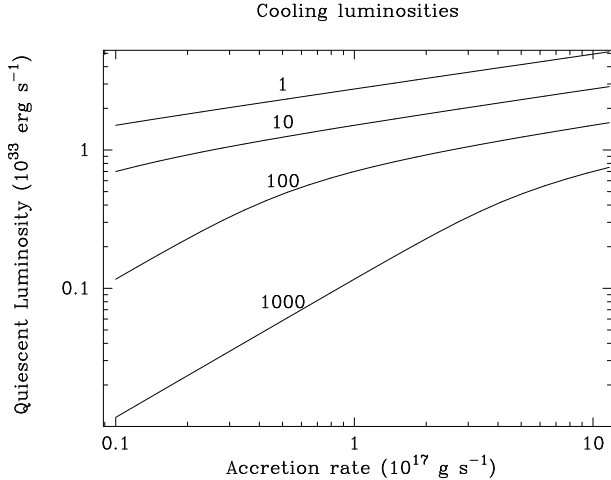


Fig. 5. Quiescent black body luminosities from a cooling neutron star in units of 10^{33} erg s^{-1} as a function of the time-average accretion rate during outburst in units of 10^{17} g s^{-1} . From top to bottom, curves refer to values of the ratio of recurrence time to the duration of an outburst $\Theta = 1, 10, 100, 1000$, respectively.

ent values of Θ . For $\Theta \lesssim 100$ the luminosity is in the range $3 \times 10^{32} - 2 \times 10^{33}$ erg s^{-1} , which is comparable to the range of luminosities observed during quiescence.

Neutron star cooling is attractive in consideration of the soft X-ray spectra observed in quiescent SXRTs. However, the most reliable determinations of the equivalent black body radii hint to smaller values than the standard $\sim 10^6$ cm neutron star radius. Moreover, the ROSAT HRI observation of a flux variation on a timescale of a few days in the quiescent flux of Cen X-4 (Campana et al. 1997) as well as the hard tails observed in Aql X-1 and Cen X-4, can hardly be reconciled with quiescent emission being powered by this mechanism alone. Note that thermal emission from neutron star cooling does not impose any relevant restriction on B and P . Therefore the possibility that this mechanism contributes with a soft and nearly steady black body like component to the quiescent emission of SXRTs remains open.

6. Spin period evolution

Different spin period histories for the neutron stars in SXRTs are possible depending on which mechanism is operating during quiescence. In the following discussion we neglect the secular decrease of the magnetic field that possibly results from accretion. If a radio pulsar is active during quiescence, then the spin period evolution is determined by the competition between the disk spin-up accretion during the outbursts (with a torque of $N = \dot{M} \sqrt{GM r_m}$) and spin-down caused by radio pulsar losses in the quiescent phases; these two effects balance for

$$B_9 \simeq 2 \times 10^{-2} P_{-2}^{187/80} L_{37}^{41/80} M_{1.4}^{-91/320} R_6^{-199/80} \Theta_{100}^{-187/320} \quad (12)$$

where L_{37} is the time-averaged outburst luminosity in units of 10^{37} erg s^{-1} and Θ_{100} the ratio between the time spent in quiescence and the average outburst duration in units of 100. SXRTs above the corresponding line in the $B - P$ diagram (see Fig. 4) would undergo secular spin-down, whereas a secular spin-up would characterise SXRTs below the line. The timescale for the period evolution is $\tau \equiv P/\dot{P} \sim 10^{10} B_9^{-2} P_{-2}^2$ yr in the case of a radio pulsar spin-down, and $\tau \sim 10^9 B_9^{-2/7} M_{1.4}^{3/7} L_{37}^{-6/7} P_{-2}^{-1}$ yr (e.g. Henrichs 1983) in the case of disk-like accretion for the same set of parameters as above. Note that the position of the equilibrium line in Fig. 4 agrees well both with the enshrouded pulsar regime described in Section 5.3 and with the region suggested by the kHz QPOs.

If the accreting matter is stopped at the magnetospheric radius during the quiescent phase, the neutron star enters the propeller regime and a pronounced spin-down results that will affect its period evolution. Different spin-down mechanisms have been proposed to describe the action of the centrifugal barrier. The spin-down torque predicted by the Illarionov & Sunyaev (1975) propeller mechanism is the same in module as for the spin-up by a disk (i.e. the torque $N = -\dot{M} \sqrt{GM r_m}$). However, the system spends a factor Θ more time in the propeller regime with an accretion rate much smaller. In this case the equilibrium does not depend on the neutron star parameters (as long as B and P are such that the neutron star remains in the propeller regime during quiescence). A net spin-down will occur if

$$L_{37} \lesssim 0.6 (L_{33}^q)^{7/9} B_9^{4/9} M_{1.4}^{1/9} R_6^{1/3} \Theta_{100}^{7/6} \quad (13)$$

(where L_{33}^q is the quiescent luminosity in units of 10^{33} erg s^{-1}). A spin-up will result if the condition above is not satisfied. The spin-up/down time scale in this regime is $\tau \sim 10^7 B_9^{-2/7} M_{1.4}^{3/7} L_{37}^{-6/7} P_{-2}^{-1}$ yr (e.g. Henrichs 1983), which is much shorter than in the case of a radio pulsar. Different versions of the propeller regime have been proposed. The (only) one relying on numerical simulations provides a much more efficient spin-down mechanism (Wang & Robertson 1985). Milder versions of the propeller mechanism have also been suggested (e.g. the supersonic propeller of Davies & Pringle 1981; Lipunov & Popov 1995). Though still highly uncertain, the modeling of the propeller effect suggests that substantial period variations of either sign can take place on relatively short timescales if quiescent SXRTs are in this regime.

7. Conclusions

The properties of SXRTs in outburst are clearly linked to those of persistent LMXRBs, as testified by e.g. their X-ray spectra, the occurrence of type I bursts, optical brightenings and kHz QPOs, indicating that SXRTs host weakly magnetic neutron stars.

For X-ray luminosities much below the outburst maxima, SXRTs show similarities with transient BHCs. In particular, as the luminosity decreases at a level of $\sim 10^{36} - 10^{37}$ erg s^{-1} in a few SXRTs (as well as in persistent LMXRBs) the X-ray spectrum shows a transition from a relatively soft thermal spectrum to a power-law like spectrum extending up to 100 keV (Barret & Vedrenne 1994; Mitsuda et al. 1989; Harmon et al. 1996). A similar spectral transition occurs also across the ‘‘high’’ and ‘‘low states’’ of several BHCs (e.g. Tanaka & Shibazaki 1996). The spectral hardening in BHCs has been

interpreted in terms of a change in the disk to an advection-dominated regime (Narayan & Yi 1995). This regime has also been invoked to explain the low luminosity emission of the BHCs A 0620–00 (Narayan, McClintock & Yi 1997) and V404 Cyg (Narayan, Barret & McClintock 1997). We note however that in the case of SXRTs the presence of a “hard surface” (either the star surface or the magnetosphere) makes the application of simple advection-dominated models questionable.

Also in quiescence, SXRTs and transient BHCs show similar properties, displaying a soft spectral component (with equivalent black body temperatures of $\sim 0.2 - 0.3$ keV; e.g. Tanaka & Shibazaki 1996). However ASCA and BeppoSAX observations of Cen X-4 (Asai et al. 1996a) and Aql X-1 (Campana et al. 1998) during quiescence demonstrated the presence of hard tails which have not been detected in BHCs.

We note also that the Aql X-1 outburst decay resembles closely the evolution of dwarf novae outbursts, with a drastic turn off of the luminosity (e.g. Osaki 1996). Models of low mass X-ray transient outbursts hosting an old neutron star or a black hole are largely built in analogy with dwarf novae outbursts. In particular, van Paradijs (1996) showed that the different range of time-averaged mass accretion rates over which the dwarf nova and low mass X-ray transient outbursts were observed to take place is well explained by the higher level of disk irradiation caused by the higher accretion efficiency of neutron stars and black holes. However, the outburst evolution of low mass X-ray transients presents important differences. In particular, the steepening in the X-ray flux decrease of Aql X-1 has no clear parallel in low mass X-ray transients containing BHCs. The best sampled light curves of these sources show an exponential-like decay (sometimes with a superposed secondary outburst) with an e -folding time of ~ 30 d and extending up to four decades in flux, with no indication of a sudden steepening (Chen, Shrader & Livio 1997). In addition, BHC transients display a larger luminosity range between outburst peak and quiescence than neutron star SXRTs (Garcia et al. 1998 and references therein). Being the mass donor stars and the binary parameters quite similar in the two cases, it appears natural to attribute these differences to the different nature of the underlying object. In principle after the decay of a neutron star SXRT outburst the X-ray emission might be dominated by different mechanisms, notably accretion onto the magnetosphere, emission from an enshrouded MSP or cooling from the neutron star surface. None of these has an equivalent in the case of BHCs.

In the case of Aql X-1 for which a spin period frequency of 2–4 ms has been inferred, accretion onto the neutron star surface during the quiescent state of SXRTs would imply a neutron star magnetic field $\lesssim 5 \times 10^6$ G. Extrapolating this result, one would conclude that SXRTs could not be among the progenitors of MSPs. Cooling of the neutron star surface can easily account for the softness of X-ray spectra. However, the observation of a flux variation on a timescale of a few days in the quiescent flux of Cen X-4 (Campana et al. 1997) can hardly be reconciled with this mechanism alone. Moreover, the observation of a hardened spectral component in Aql X-1 (Campana et al. 1998) and Cen X-4 (Asai et al. 1996a) poses problems to accretion onto the surface and cooling mechanisms.

Accretion onto the neutron star magnetosphere is one interesting possibility to explain the quiescent emission of SXRTs. If this regime applies, the allowed region in the $B - P$ diagram, even if far from MSPs near the Eddington spin-up line,

contains a relevant number of MSPs and straddles the region where neutron stars of LMXRBs are expected to lie. The spin period evolution in this case is mainly dictated by the ratio of the mean luminosity in outburst and during quiescence, so that either spin-up and spin-down are possible, even if a secular spin-down is more likely (cf. Eq. 13).

Shock emission powered by an underlying MSP is the other plausible mechanism for the quiescent emission of SXRTs. In this regime, SXRTs would occupy a region in the $B - P$ diagram containing a large number of MSPs and likely including kHz QPO sources. The equilibrium line between spin-up during outburst and spin-down due to radiative losses in quiescence, lies just in the middle of the expected neutron star spin-down luminosities. BeppoSAX observations of Aql X-1 provide the best evidence so far for this mechanism (Campana et al. 1998). The predicted spectrum show a substantial flux at energies beyond the soft (e.g. ROSAT) energy range. However, a soft component is present in all SXRTs detected in quiescence, so that other components have to be invoked, like a more complex shock emission mechanism or the contribution from the cooling neutron star.

For the pulsar shock emission regime to apply, the closure of the centrifugal barrier must take place at a level of $\sim 10^{36}$ erg s $^{-1}$ (cf. Eq. 4), with a small jump in luminosity (cf. Eq. 7), as observed in Aql X-1. This is also the range of luminosities characterising the spectral hardening observed in persistent LMXRBs and SXRTs. This spectral change has been indeed related to the transition to the propeller regime in the case of Aql X-1 (Zhang, Yu & Zhang 1998; Campana et al. 1998). In this interpretation SXRTs represent the immediate progenitors of MSPs.

Estimating the current number of SXRTs in our Galaxy is not an easy task, due to the presence of strong selection effects (e.g. large column densities along the galactic plane; lower peak luminosities with respect to BHCs; limited temporal coverage, etc.). A likely number is a few hundreds for mean recurrence time of ~ 10 yr and about a thousand for a recurrence time of ~ 50 yr (Tanaka & Shibazaki 1996).

Despite the recent discoveries on Aql X-1 by RossiXTE and BeppoSAX, deeper studies are necessary to better assess the nature of the neutron stars in SXRTs. The case of Aql X-1 emphasises the importance of combining the nearly continuous monitoring of the outburst evolution that can be obtained by large field X-ray instruments, with deeper and more detailed pointed observations by narrow field X-ray telescopes during the crucial phases of the outbursts.

Note added in proof.

After this paper was accepted for publication, we became aware that in April 1998 RXTE revealed a transient X-ray source at a position consistent with SAX J1808.4–3658 (in’t Zand et al. 1998), a variable X-ray burster in the direction of the galactic bulge. During pointed RXTE observations highly significant coherent pulsations at ~ 401 Hz were detected. These allowed also to measure an orbital period of ~ 2 hr and a mass function of $\sim 4 \times 10^{-5} M_{\odot}$ (Wijnands & van der Klis 1998; Chakrabarty & Morgan 1998).

These results show that SAX J1808.4–3658 is a LMXRB, the first to show coherent millisecond pulsations in its persistent emission. A radio pulsar (perhaps a partially eclipsing one) might turn on after the X-ray outburst ends. In any case SAX J1808.4–3658 further strengthens the link between SXRTs and MSPs.

Acknowledgement. We thank an anonymous referee for providing useful comments. This work was partially supported through ASI grants.

References

- Alpar M.A., Cheng A.F., Ruderman M.A. & Shaham J., 1982, Nat 300 728
- Alpar M.A. & Shaham J., 1985, Nat 316 239
- Angelini L., Stella L. & Parmar A.N., 1989, ApJ 346 906
- Aoki K. et al., 1992, PASJ 44 641 (4)
- Arons J. & Tavani M., 1993, ApJ 403 249
- Asai K. et al., 1996a, PASJ 48 257 (5)
- Asai K. et al., 1996b, PASJ 48 L21 (8)
- Backer D.C., Kulkarni S.R., Heiles C., Davis M.M. & Goss W.M., 1982, Nat 300 615
- Barr P. et al., 1987, A&A 176 69
- Barret D. & Vedrenne G., 1994, ApJS 92 505
- Barret D. et al., 1992, ApJ 394 615 (10)
- Belloni T. et al., 1993, A&A 271 487
- Berger M. et al., 1996, ApJ 469 L13
- Bhattacharya D. & van den Heuvel E.P.J., 1991, Phys. Rep. 203 1
- Biggs J.D. & Lyne A.G., 1996, MNRAS 282 691
- Biggs J.D., Lyne A.G. & Johnston S., 1989, in *23rd ESLAB Symp. on two topics in X-Ray Astronomy*, eds. J. Hunt & B. Battrick, ESA SP-296, p 293
- Björnsson C.-I., 1996, ApJ 471 321
- Bouchacourt P. et al., 1984, ApJ 285 L67
- Branduardi G., Ives J.C., Sanford P.W., Brinkman A.C. & Maraschi L., 1976, MNRAS 175 47
- Brookshaw L. & Tavani M., 1995, in *Millisecond Pulsars: A Decade of Surprise*, eds. A. Fruchter, M. Tavani & D.C. Backer (San Francisco: ASP), p 244
- Campana S., Colpi M., Mereghetti S. & Stella L., 1996, in *Röntgenstrahlung from the universe*, eds. H.U. Zimmermann, J.E. Trümper & H. Yorke, MPE report 263, p 127
- Campana S., Mereghetti S., Stella L. & Colpi M., 1997, A&A 324 941
- Campana S. et al. 1998, ApJL in press (16)
- Canizares C.R., McClintock J.E. & Grindlay J.E., 1979, ApJ 234 556
- Cannizzo J.K., 1993, in *Accretion Disks in Compact Stellar Systems*, ed. J.C. Wheeler, World Scientific Publishing, Singapore, p 6
- Cannizzo J.K., Chen W. & Livio M., 1995, ApJ 454 880
- Casares J., Charles P.A. & Naylor T., 1992, Nat 355 614
- Chakrabarty D. & Morgan E.H., 1998, Nature submitted
- Chen K. & Ruderman M., 1993, ApJ 402 264
- Chen W., Shrader C.R. & Livio M., 1997, ApJ 491 312
- Chevalier C. & Ilovaisky S.A., 1991, A&A 251 L11
- Chevalier C. & Ilovaisky S.A., 1997, IAUC N.6806
- Chevalier C., Ilovaisky S.A., van Paradijs J., Pedersen H. & van der Klis M., 1989, A&A 210 114
- Cominsky L., Jones C., Forman W. & Tananbaum H., 1978, ApJ 224 46
- Cominsky L., Ossmann W. & Lewin W.H.G., 1976, ApJ 270 226
- Cominsky L. & Wood K.S., 1984, ApJ 283 765 (7)
- Conner J.P., Evans W.D. & Belian R.D., 1969, ApJ 157 L157
- Corbet R.H.D., 1996, ApJ 457 L31
- Corbet R.H.D., Asai K., Dotani T. & Nagase F., 1994, ApJ 436 L15
- Cordes J.M., Romani R.W. & Lundgren S.C., 1993, Nat 362 133
- Cowley A.P., Hutchings J.B., Crampton D., Schmidtke P.C. & Hartwick F.D.A., 1988, AJ 95 1231
- Czerny M., Czerny B. & Grindlay J.E., 1987, ApJ 312 122
- Davies R.E. & Pringle J.E., 1981, MNRAS 196 209
- Davis R.D., Walsh D., Browne I.W.A., Edwards M.R. & Noble R.G., 1976, Nat 261 476
- Dempsey R.C., Linsky J.L., Fleming T.A. & Schmitt J.H.M.M., 1995, ApJS 86 599
- Fabbiano G. et al., 1978, ApJ 221 L49
- Ford E. et al., 1997, ApJ 475 L123
- Ford E., van der Klis M. & Kaaret P., 1998, ApJL in press
- Forman W., Jones C. & Tananbaum H., 1976, ApJ 207 L25
- Forman W. et al., 1978, ApJS 38 35
- Fruchter A., Bookbinder J., Garcia M.R. & Bailyn C.D., 1992, Nat 359 303
- Fujimoto M.Y., Hanawa T., Iben I.Jr. & Richardson M.B., 1984, ApJ 278 813
- Garcia M.R., 1994, ApJ 435 497
- Garcia M.R., Bailyn C.D., Grindlay J.E. & Molnar L.A., 1989, ApJ 341 L75
- Garcia M.R. & Callanan P.J., 1998, ApJ submitted (3)
- Garcia M.R., McClintock J.E., Narayan R. & Callanan P.J., 1998, in *Proceedings of the 13th North American Workshop on CVs*, eds. S. Howell, E. Kuipers & C. Woodward, San Francisco AIP, in press
- Ghosh P., 1995, ApJ 453 411
- Ghosh P. & Lamb F.K., 1979a, ApJ 232 259
- Ghosh P. & Lamb F.K., 1979b, ApJ 234 296
- Ghosh P. & Lamb F.K., 1992, in *X-ray binaries and recycled pulsars*, eds. E.P.J. van den Heuvel & S.A. Rappaport, Kluwer, p 487 (GL92)
- Grindlay J.E., 1981, in *X-ray astronomy with the Einstein satellite*, ed. R. Giacconi (Reidel, Dordrecht), p 79
- Grindlay J.E., 1994, Mem SAI 65 259
- Grindlay J.E. & Liller W., 1978, ApJ 220 L127
- Grove J.E. et al., 1995, ApJ 447 L113
- Gudmundsson E.H., Pethick C.J. & Epstein R.I., 1983, ApJ 272 286
- Guerriero R., Lewin W.H.G. & Kommers J., 1997, IAUC N.6689
- Hameury J.M., King A.R. & Lasota J.P., 1986, A&A 162 71
- Harmon B.A. et al., 1996, A&AS 120 197
- Hasinger G. & van der Klis M., 1989, A&A 225 79
- Henrichs H.F., 1983, in *Accretion-driven stellar X-ray sources*, eds. W.H.G. Lewin & E.P.J. van den Heuvel (Cambridge Univ. Press), p 393
- Hertz P. & Grindlay J.E., 1983, ApJ 275 105
- Hjellming R.M., Han X. & Roussel-Duprè D., 1990, IAUC N.5112
- Hjellming R.M. et al., 1988, ApJ 335 L75
- Huang M. & Wheeler J.C., 1989, ApJ 343 229
- Illarionov A.F. & Sunyaev R.A., 1975, A&A 39 185
- in't Zand J.J.M. et al., 1989, in *The 23rd ESLAB Symposium on Two Topics in X Ray Astronomy*, eds. J. Hunt & B. Battrick, ESA SP-296, p 693
- in't Zand J.J.M. et al., 1998, A&A 331 L25 (15)
- Johnston H.M., Verbunt F. & Hasinger G., 1995, A&A 298 L21
- Jones T.W. & Hardee P.E., 1979, ApJ 228 268
- Jonker P. et al., 1998, ApJL in press

- Kaluzienski L.J., Holt S.S. & Swank J.H., 1980, ApJ 241 779
- Kaspi V. et al., 1995, ApJ 453 424
- Kennea J.A. & Skinner G.K., 1996, PASJ 48 L117
- Kennel C.F. & Coroniti F.V., 1984, ApJ 283 694
- Kitamoto S., Tsunemi H., Miyamoto S. & Roussel-Duprè D., 1993, ApJ 403 315
- Koyama K. et al., 1981, ApJ 247 L27
- Kulkarni S.R. & Hester J.J., 1988, Nat 335 801
- Kulkarni S.R., Narayan R. & Romani R.W., 1990, ApJ 356 174
- Kulkarni S.R., Navarro J., Vasisht G., Tanaka Y., & Nagase F., 1992, in *X-ray binaries and recycled pulsars*, eds. van den Heuvel E.P.J. & Rappaport S.A., Kluwer, p 99
- Lamb F.K., Shibazaki N., Alpar M.A. & Shaham J., 1985, Nat 317 681
- Lasota J.P., 1995, in *Compact Stars in Binaries*, IAU Symposium 165, eds. E.P.J. van den Heuvel & J. van Paradijs, Kluwer
- Levine A.M., Garcia A., Berlind P. & Callanan P., 1997, IAU Circ. No. 6558
- Levine A.M. et al., 1984, ApJS 54 581
- Lewin W.H.G., Hoffman J.A. & Doty J., 1976a, IAUC N.2994
- Lewin W.H.G., van Paradijs J. & Taam R.E., 1993, SSRv 62 233
- Lewin W.H.G., van Paradijs J. & Taam R.E., 1995, in *X-ray binaries*, eds. W.H.G. Lewin, J. van Paradijs & E.P.J. van den Heuvel, (Cambridge Univ. Press), p 175
- Lewin W.H.G. et al., 1976b, IAUC N.2922
- Lewin W.H.G. et al., 1978, IAUC N.3190
- Li J. & Wickramasinghe D.T., 1996, MNRAS 286 P25
- Lipunov V.M., 1992, *Astrophysics of neutron stars*, Springer Verlag
- Lipunov V.M. & Popov S.B., 1995, Astr. Rep. 39 632
- Lochner J.C. & Roussel-Duprè D., 1994, ApJ 435 840 (6)
- Lyne A.G. et al., 1990, Nat 347 650
- Maeda Y., Koyama K., Sakano M. Takeshima T. & Yamauchi S., 1996, PASJ 48 417 (11)
- Manchester R.N., Lyne A.G., Robinson C., Bailes M. & D'Amico N., 1991, Nat 352 219
- Maraschi L. & Cavaliere A., 1977, in *Highlights in Astronomy*, ed. E.A. Muller (Reidel, Dordrecht), vol.4, Part I, p. 127
- Maraschi L., Treves A. & van den Heuvel E.P.J., 1976, Nat 259 292
- Markert T.H., Backman D.E., Canizares C.R., Clark G.W. & Levine A.M., 1975, Nat 257 32
- Markert T.H. et al., 1977, ApJ 218 801
- Marshall F.E. & Angelini L., 1996, IAUC N.6331
- Matsuoka M. et al., 1980, ApJ 240 L137
- McClintock J.E. & Remillard R.A., 1986, ApJ 308 110
- McClintock J.E. & Remillard R.A., 1990, ApJ 350 386
- Mendez M. et al., 1998, ApJ 494 L65
- Meyer F. & Meyer-Hofmeister E., 1983, A&A 121 29
- Miller M.C., Lamb F.K. & Psaltis D., 1998, ApJ in press
- Mineshige S. & Wheeler J.C., 1989, ApJ 343 241
- Miralda-Escudé J., Paczyński B. & Haensel P., 1990, ApJ 362 572
- Mitsuda K., Inoue H., Nakamura N. & Tanaka Y., 1989, PASJ 41 97
- Molnar L.A. & Neely M., 1992, IAUC N.5595
- Murakami T. et al., 1980, PASJ 32 543
- Narayan R., Barret D. & McClintock J.E., 1997, ApJ 482 448
- Narayan R., McClintock J.E. & Yi I., 1996, ApJ 457 821
- Narayan R. & Yi I., 1995, ApJ 452 710
- Orsoz J.E., Bailyn C.D., McClintock J.E. & Remillard R.A., 1996, ApJ 468 380
- Osaki Y., 1985, A&A 144 369
- Osaki Y., 1996, PASP 108 390
- Parmar A.N., Smale A.P., Verbunt F. & Corbet R.D.H., 1991, ApJ 366 253
- Parmar A.N., White N.E., Giommi P. & Gottwald M., 1986, ApJ 308 199 (2)
- Parmar A.N., White N.E. & Stella L., 1989, ApJ 338 373
- Parmar A.N. et al., 1989, ApJ 338 359
- Penninx W., Damen E., van Paradijs J., Tan J. & Lewin W.H.G., 1989, A&A 208 146
- Petro L.D., Bradt H.V., Kelley R.L., Horne K. & Gomer R., 1981, ApJ 251 L7
- Phinney E.S. & Kulkarni S.R., 1994, ARA&A 32 591
- Pietsch W., Steinle H., Gottwald M. & Graser U., 1986, A&A 157 23
- Predehl P., Hasinger G & Verbunt F., 1991, A&A 246 L21 (14)
- Priedhorsky W.C., 1986, ApJ 306 L97
- Priedhorsky W.C. & Terrell J., 1984, ApJ 280 661
- Proctor R.J., Skinner G.K. & Willmore A.P., 1978, MNRAS 185 745 (12)
- Rudak B. & Ritter H., 1994, MNRAS 267 513
- Ruderman M. & Sutherland P., 1975, ApJ 196 51
- Rutledge R. et al., 1998, IAUC N.6813
- Schoelkopf R.J. & Kelley R.L., 1991, ApJ 375 696
- Shaham J. & Tavani M., 1991, ApJ 377 588
- Shahbaz T., Casares J. & Charles P.A., 1997, A&A 326 L5
- Shahbaz T., Naylor T. & Charles P.A., 1993, MNRAS 265 655
- Shahbaz T. et al., 1996, MNRAS 282 1437
- Shakura, N.I. & Sunyaev, R.A., 1973, A&A 24 337
- Share G. et al., 1978, IAUC N.3190
- Smak J.I., 1984, Acta Astron. 34 161
- Smale A.P., Zhang W.W. & White N.E., 1997, ApJ 483 L119
- Smith D.A., Morgan E.H. & Bradt H., 1997, ApJ 479 L137
- Srinivasan G., 1989, A&ARv 1 209
- Stella L., Campana S., Colpi M., Mereghetti S. & Tavani M., 1994, ApJ 423 L47 (Paper I)
- Stella L., White N.E. & Rosner R., 1986, ApJ 308 669
- Strohmayer T.E. et al., 1996, ApJ 469 L9
- Sunyaev R.A., 1989, IAUC N.4839
- Sunyaev R.A. et al., 1990, AdSpR 11 13
- Sunyaev R.A. et al., 1991, AdSpR 11 177
- Tamura K., Tsunemi H., Kitamoto S., Hayashida K. & Nagase F., 1992, ApJ 389 676
- Tanaka Y., 1994, in *New Horizon of X-ray Astronomy*, eds. F. Makino & T. Ohashi (Tokio, Universal Acad.), p 37
- Tanaka Y. & Shibazaki N., 1996, ARA&A 34 607
- Tavani M., 1991, ApJ 379 L69
- Tavani M. & Arons J., 1997, ApJ 477 439
- Tavani M. & Brookshaw L., 1991, ApJ 381 L21
- Tavani M. & Brookshaw L., 1993, A&A 267 L1
- Taylor J.H., Manchester R.N. & Lyne A.G., 1993, ApJS 88 529
- Thomas B., Corbet R., Smale A., Asai K. & Dotani T., 1997, ApJ 480 L21
- Thorstensen J., Charles P. & Bowyer S., 1978, ApJ 220 L131
- Thorstensen J. et al., 1979, ApJ 233 L57
- Trudolyubov S. et al., 1996, in *Röntgenstrahlung from the universe*, eds. H.U. Zimmermann, J.E. Trümper & H. Yorke, MPE report 263, p 201 (9)
- van der Klis M., 1995, in *X-ray binaries*, eds. W.H.G. Lewin, J. van Paradijs & E.P.J. van den Heuvel (Cambridge Uni-

versity Press), p 252

van der Klis M., 1997, in *The many faces of neutron stars* Proc. NATO-ASI, eds. A. Alpar, L. Buccheri, & J. van Paradijs (Dordrecht: Kluwer), in press

van der Klis M., 1998, in *The Active X-ray Sky: Results from Beppo-SAX and Rossi-XTE*, Nuclear Physics B Proceedings Supplements, eds. L. Scarsi, H. Bradt, P. Giommi & F. Fiore, in press

van der Klis M. et al., 1996, IAUC 6511

van der Klis M., Wijnands R.A.D., Horne K. & Chen W., 1997, ApJ 481 L97

van Paradijs J., 1996, ApJ 464 L139

van Paradijs J. & McClintock J.E., 1994, A&A 290 133

van Paradijs J. & McClintock J.E., 1995, in *X-ray binaries*, eds. W.H.G. Lewin, J. van Paradijs & E.P.J. van den Heuvel, (Cambridge Univ. Press), p 58

van Paradijs J., Verbunt F., Shafer R.A. & Arnaud K.A., 1987, A&A 182 47

van Paradijs J. & White N.E., 1995, ApJ 447 L33

Vaughan B.A. et al., 1994, ApJ 435 362

Verbunt F., 1996, IAU Symp. 165, ed. E.P.J. van den Heuvel, p 333

Verbunt F., Belloni T., Johnston H., van der Klis M. & Lewin W.H.D., 1994b, A&A 285 903

Verbunt F., Johnston H., Hasinger G., Belloni T. & Bunk W., 1994a, Mem SAIt 65 249

Verbunt F. et al., 1996, A&A 311 L9

Wachter S., 1997, ApJ 485 839

Wang Y.-M., 1987, A&A 183 257

Wang Y.-M., 1995, ApJ 449 L153

Wang Y.-M., 1996, ApJ 465 L111

Wang Y.-M. & Robertson J.A., 1985, A&A 151 361

Warwick R.S., Norton A.J., Turner M.J.L., Watson M.G. & Willingale R., 1988, MNRAS 232 551 (13)

Watson M.G. & Ricketts M.J., 1978, MNRAS 183 P35 (1)

White N.E., 1989, ARA&A 1 85

White N.E. & Holt S.S., 1982, ApJ 257 318

White N.E., Kaluzienski J.L. & Swank J.H., 1984, in *High Energy Transients in Astrophysics*, ed. S.E. Woosley, AIP Conf. Proc. 115, p 31

White N.E. & Marshall F.E., 1984, ApJ 281 354

White N.E. & Stella L., 1988, MNRAS 231 325

Wijnands R.A.D., Homan J, van der Klis M. et al., 1998c, ApJL in press

Wijnands R.A.D. & van der Klis M., 1997, ApJ 482 L65

Wijnands R.A.D. & van der Klis M., 1998, Nature submitted

Wijnands R.A.D. et al., 1998a, ApJ 495 L39

Wijnands R.A.D. et al., 1998b, ApJ 493 L87

Wijnands R.A.D. et al., 1997, ApJ 479 L141

Yu W. et al., 1997, ApJ 490 L153

Zampieri L., Turolla R., Zane S. & Treves A., 1995, ApJ 439 849

Zel'dovich Ya. & Shakura N., 1969, Soviet Astron.-AJ 13 175

Zhang S.N., Lapidus I., White N.E. & Titarchuk L., 1996a, ApJ 469 L17

Zhang S.N., Yu W. & Zhang W.W., 1998, ApJ 494 L71

Zhang S.N. et al., 1996b, A&AS 120 279

Zhang W.W. et al., 1998, ApJ 495 L9

A. Ghosh and Lamb threaded-disk model

In Section 4 we considered the case of spherical accretion, however an accretion disk most likely forms during SXRT outbursts as a consequence of the high specific angular momentum of the accreting matter. Several models have been proposed for the interaction between the accreting disk matter and the magnetosphere of a neutron star (White & Stella 1988). Here we consider the model described by Ghosh & Lamb (1992 and references therein, hereafter GL92). In this model the neutron star magnetic field penetrates the disk over a relatively large range of radii and two regions can be distinguished: an outer transition zone, with a small coupling between matter and magnetic field, and a narrow inner zone with the character of a boundary layer, in which matter is brought to corotation by the magnetic field. GL92 adopted a time-averaged description, taking a standard Shakura-Sunyaev disk (Shakura & Sunyaev 1973) and introducing an effective electrical conductivity in order to describe the magnetohydrodynamic interaction between matter and magnetic field.

Solving a set of radial and vertical disk structure equations, together with Maxwell's equations, GL92 derived the magnetospheric radius in a gas pressure-dominated accretion disk:

$$r_m^{GL} = 5 \times 10^6 \dot{M}_{15}^{-46/187} B_9^{108/187} M_{1.4}^{-41/187} R_6^{324/187} \text{ cm} \quad (14)$$

In order to account for the torque exerted by magnetic field lines onto the accreting matter, Ghosh & Lamb (1979a; 1979b) introduced the ‘‘fastness’’ parameter $\omega = \Omega_*/\Omega_k(r_m)$, with Ω_* the angular frequency of the neutron star and $\Omega_k(r_m)$ the angular frequency of the inner edge of the disk. We consider here as the condition for the location of the centrifugal barrier $r_m \lesssim r_{\text{cor}}(\omega_c)^{2/3}$, where ω_c is the critical value of ω for which the torque exerted by the accretion disk on the neutron star vanishes.

Different values have been proposed for ω_c (GL92; Wang 1995, 1996). Following Li & Wickramasinghe (1996) we adopt $\omega_c \sim 0.5$. With this prescription, the minimum accretion-induced luminosity onto the neutron star surface can be written as:

$$L_{\text{min}}^{GL} \sim 10^{35} B_9^{54/23} M_{1.4}^{-86/69} R_6^{139/23} P_{-2}^{-187/69} \omega_{c,0.5}^{-187/69} \text{ erg s}^{-1} \quad (15)$$

where also the factor of 1/2 has been included (see Section 4). When the centrifugal barrier closes a decrease in the luminosity is predicted down to

$$L^{GL}(r_{\text{cor}}) \sim 9 \times 10^{33} B_9^{54/23} M_{1.4}^{-109/69} R_6^{162/23} P_{-2}^{-233/69} \omega_{c,0.5}^{-187/69} \text{ erg s}^{-1} \quad (16)$$

(compare this value with the one derived in the spherical free-fall approximation, cf. Eq. 3). If the accretion rate decreases further the magnetospheric radius can become comparable to the light cylinder radius. If this happen the radio pulsar mechanism can turn on and start sweeping the infalling matter away. In the case of an accretion disk with a boundary layer modeled following GL92, this occurs at a luminosity of

$$L^{GL}(r_{\text{lc}}) \sim 9 \times 10^{29} B_9^{54/23} M_{1.4}^{5/46} R_6^{162/23} P_{-2}^{-233/46} \omega_{c,0.5}^{-187/69} \text{ erg s}^{-1} \quad (17)$$

Ghosh–Lamb disk accretion

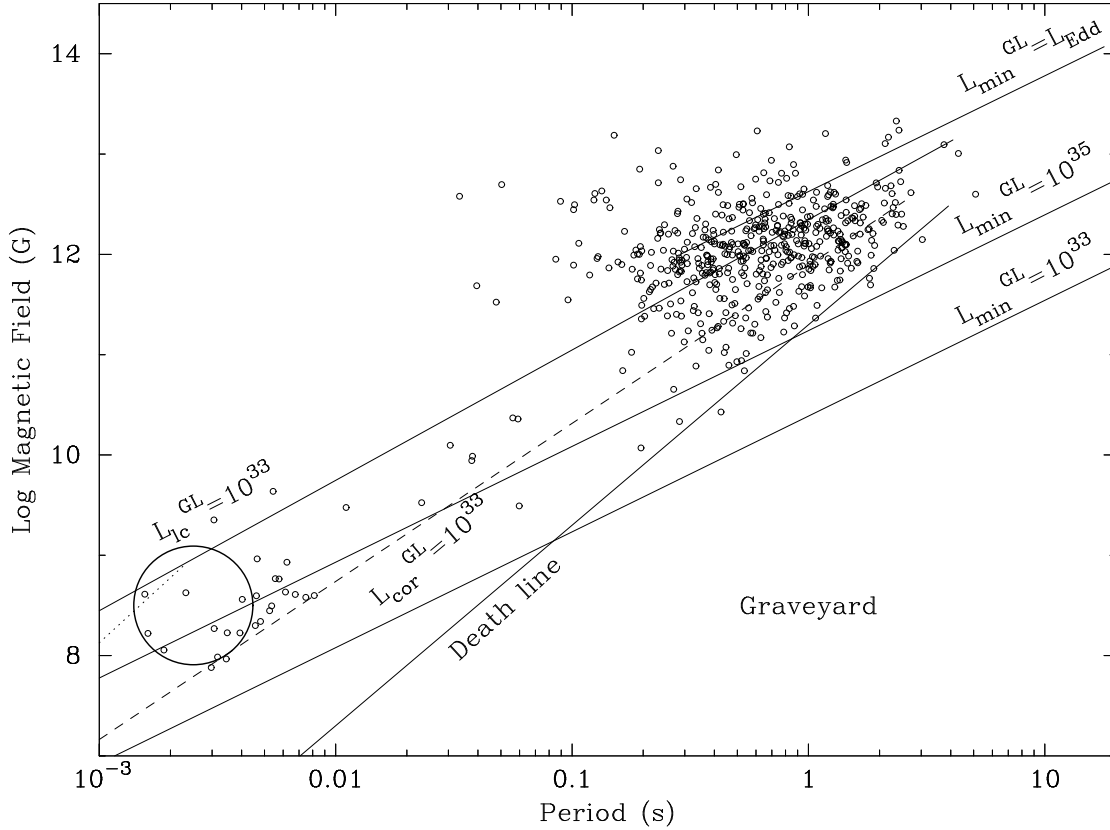


Fig. 6. Surface magnetic field plotted versus spin period of known pulsars (circles). Solid lines represent the spin-up lines for threaded-disk accretion given by Eq. 15. The line corresponding to the Eddington luminosity has been calculated either for the gas pressure-dominated (lower part) and for the radiation pressure-dominated (upper part) threaded-disk. The dotted lines indicate the maximum luminosity that can be released in the propeller regime (cf. L_{cor}^{GL}) and the dashed line the minimum luminosity (cf. L_{lc}^{GL}). The large circle in the millisecond period-low magnetic field region includes the kHz QPO sources.

We have described only the gas pressure-dominated case in the region b of a Shakura-Sunyaev disk, where the Thomson opacity dominates over the free-free one. Ghosh & Lamb have not worked out the case of the region c , whereas the case of the radiation pressure-dominated region a , the magnetospheric radius provided in GL92 is

$$r_m^A = 3 \times 10^6 B_9^{20/39} \dot{M}_{17}^{-2/13} M_{1.4}^{-5/39} R_6^{20/13} \text{ cm} \quad (18)$$

The relevant luminosities can then be easily derived:

$$L_{\text{min}}^{GL,A} = 6 \times 10^{35} B_9^{10/3} M_{1.4}^{-2} R_6^9 P_{-2}^{-13/3} \omega_{c,0.5}^{-13/3} \text{ erg s}^{-1} \quad (19)$$

$$L^{GL,A}(r_{\text{cor}}) = 4 \times 10^{34} B_9^{10/3} M_{1.4}^{-7/3} R_6^{10} P_{-2}^{-5} \omega_{c,0.5}^{-13/3} \text{ erg s}^{-1} \quad (20)$$

$$L^{GL,A}(r_{\text{lc}}) = 5 \times 10^{28} B_9^{10/3} M_{1.4}^{1/6} R_6^{10} P_{-2}^{-15/2} \omega_{c,0.5}^{-13/3} \text{ erg s}^{-1} \quad (21)$$

A.1. A comparison between spherical and disk accretion models

As apparent from Eqs. 1 and 14 the accretion flow is dominated by the neutron star magnetic field within a radius, r_m , the magnitude of which depends sensitively on the geometry of the inflow. The ratio of the magnetospheric radius in the spherical and disk geometry as a function of the accretion rate is given by

$$\frac{r_m^{sp}}{r_m^{GL}} \sim 3 \dot{M}_{17}^{-52/1309} B_9^{-8/1309} M_{1.4}^{100/1309} R_6^{-24/1309} \quad (22)$$

As a consequence of this the minimum accretion-induced X-ray luminosity in the spherical case exceeds the corresponding value in the disk case by a factor of ~ 10 (for $B = 10^9$ G and $P = 10$ ms). In turn this causes the lines of constant minimum luminosity L_{min} in the disk case to move upwards in the $B-P$ diagram, allowing for higher magnetic fields and smaller spin periods. This is clearly seen in Figs. 3 and 6. If a radio pulsar were to be present in a SXRT at the end of disk accretion such radio pulsar can have a higher spin-down luminosity.

Application of the standard beat-frequency model (Alpar & Shaham 1985) to bright X-ray pulsars led Wang (1995) to conclude that the neutron star's dipole field fully or almost fully

threads the disk. This would imply that the magnetospheric radius obtained in the case of spherical accretion is very similar to the one for disk accretion.

B. Cooling neutron star model

In this Appendix, we describe a simple model for the thermal evolution of a neutron star in SXRTs. Our aim is to determine the core temperature T_c (and in turn the surface radiation temperature T_s) of the neutron star heated up by nuclear energy deposition that takes place during the accretion episodes that give rise to the outbursts. First, we verify that the evolution equation for T_c reproduces known results and later estimate how recurrent event of accretion modify T_c and the corresponding black body luminosity. In the neutron star, we distinguish a uniform core at nuclear densities and an envelope that surrounds it: energy is exchanged across the two regions and such a flow determines the equilibrium core temperature and T_s , as described below.

The core is characterised by a single temperature T_c , owing to the high conductivity of degenerate neutrons. T_c evolves according to the equation

$$C_c \frac{dT_c}{dt} = L_N - L_\nu - Q \quad (23)$$

where $C_c \sim 2 \times 10^{38} M_{1.4} T_{c,8} \text{ erg K}^{-1}$ is the heat capacity of the core and $T_{c,8}$ is its temperature in units of 10^8 K. In Eq. 23, L_N is the energy released per unit time by stable hydrogen burning ignited at the base of the envelope. At this boundary a steep inversion of the temperature gradient arises, causing the energy produced to flow into the core. As a consequence of this effect (see Fujimoto et al. 1984 and Miralda-Escudé, Paczyński & Haensel 1990 for details) L_N enters Eq. 23 as the source of heat for the core, and can be estimated as

$$L_N \sim \chi \dot{M} c^2 \sim 6 \times 10^{35} \chi_{-3} \dot{M}_{17} \text{ erg s}^{-1} \quad (24)$$

where $\chi = \chi_{-3} 10^{-3}$ is the efficiency of nuclear burning and \dot{M}_{17} is the accretion rate in units of 10^{17} g s^{-1} . Neutrino emission enters instead as a cooling term and can be estimated by considering nucleon-nucleon scattering as the dominant process (modified URCA)

$$L_\nu \sim 7 \times 10^{31} T_{c,8}^8 M_{1.4} \text{ erg s}^{-1} \quad (25)$$

Additional neutrino losses occur if a pion condensate is present in the core. Q is a cooling term representing the energy flux transferred outwards from the core to the surface via electron conduction across the stellar envelope. Following Gudmundsson, Pethick & Epstein (1983) we approximate $Q \sim 4 \times 10^{16} T_{c,8}^2 \text{ erg s}^{-1}$.

During thermal evolution, each process influences the changes in the temperature on a characteristic time scale $\tau \sim T/\dot{T}$. In the core we are led to distinguish three time scales associated to nuclear heating, neutrino and radiation cooling, respectively. We have

$$\tau_N \sim \frac{C_c T_c}{L_N} \sim 7 \times 10^3 T_{c,8}^2 \dot{M}_{17}^{-1} \chi_{-3}^{-1} M_{1.4} \text{ yr} \quad (26)$$

$$\tau_\nu \sim \frac{C_c T_c}{L_\nu} \sim 8 \times 10^6 T_{c,8}^{-6} \text{ yr} \quad (27)$$

$$\tau_{k,core} \sim \frac{C_c T_c}{Q} \sim 10^6 \text{ yr} \quad (28)$$

In the absence of accretion ($\dot{M} = 0$), Eq. 23 reproduces the evolution of an isolated neutron stars cooling by neutrino and photon emission. The energy flux across the envelope fixes the surface temperature T_s which is determined uniquely by T_c ; the resulting value is $T_{s,6} \sim 0.9 T_{c,8}^{1/2}$ and corresponding to a black body luminosity of

$$L_s \sim 7 \times 10^{32} T_{s,6}^4 \text{ erg s}^{-1} \quad (29)$$

where $T_{s,6}$ denotes the surface temperature in units of 10^6 K.

In the case of steady accretion, nuclear reaction are ignited stably and the core heats on the time scale $\sim \tau_N$. Thermal equilibrium is attained approximately when $L_\nu \sim L_N$ yielding an equilibrium temperature

$$T_{c,8}^{eq} \sim 2 \dot{M}_{17}^{1/8} \chi_{-3}^{1/8} M_{1.4}^{-1/8} \quad (30)$$

This value is close to the one found by Fujimoto et al. (1984) and Miralda-Escudé, Paczyński & Haensel (1990) using a more realistic model. If there exists a pion condensate in the interior, the equilibrium temperature would attain a lower value due to the enhanced neutrino energy losses that occur at a rate $L_{\nu,\pi} \sim 2 \times 10^{40} T_{c,8}^6 M_{1.4} \text{ erg s}^{-1}$. The inferred equilibrium temperature is in this case $T_{c,8}^{eq} \sim 0.13 \dot{M}_{17}^{1/6} \chi_{-3}^{1/6} M_{1.4}^{-1/6}$.

If at the onset of accretion $T_c \ll T_c^{eq}$, the time necessary for the core to attain equilibrium can be determined by integrating the equation $\dot{T}_c = T_c/\tau_N$, having neglected both cooling terms. The solution for $T_c(t) \propto t^{1/2}$ gives a characteristic time for equilibrium

$$t_{c,eq} \sim 2 \times 10^4 \dot{M}_{17}^{-3/4} \chi_{-3}^{-3/4} M_{1.4}^{3/4} \text{ yr} \quad (31)$$

However, our neglect of Q is justified only if the time for radiative cooling through the envelope $\tau_{k,core}$ is much longer than $t_{c,eq}$, a condition fulfilled when the steady accretion rate (averaged over the quiescence time) $\dot{M}_{17} > 3 \times 10^{-3} \chi_{-3}^{-1} M_{1.4}$. In this case the envelope behaves mainly as an “insulating” layer. This estimate is close to the limiting accretion rate below which no stable hydrogen burning can occur (Miralda-Escudé, Paczyński & Haensel 1990) and, hence, the deposition of energy into the core is completely negligible.

In a SXRTs where accretion is intermittent hydrogen burning can occur only during outbursts. In this case, energy is injected into the core during the sporadic events of accretion. Equilibrium is therefore attained on a time scale that can exceed $\tau_{k,core}$. The leakage of heat across the envelope may result in a much lower equilibrium temperature, and in turn a much lower black body luminosity.

Since $\tau_{k,core}$ is much longer than the expected recurrence time between outbursts we can estimate approximately T_c^{eq} solving Eq. 23 for a time averaged accretion rate $\dot{M} \sim \dot{M}_{SXRT}/\Theta$, where \dot{M}_{SXRT} is the mean accretion rate during outburst. For $\Theta \gtrsim 100$, the equilibrium time is found to increase significantly from the value for steady accretion of 10^4 yr to 10^7 yr, because of the leakage during quiescence.